the plant journal

SEB Society for Experimental Biology

The Plant Journal (2018) **94,** 595–611 doi: 10.1111/tpj.13880

Vacuolar Protein Sorting 26C encodes an evolutionarily conserved large retromer subunit in eukaryotes that is important for root hair growth in *Arabidopsis thaliana*

Suryatapa Ghosh Jha[1], Emily R. Larson[1,†], Jordan Humble[1], David S. Domozych[2], David S. Barrington[1] and Mary L. Tierney[1,*]

[1]*Department of Plant Biology, University of Vermont, Burlington, Vermont 05405, USA, and*
[2]*Skidmore College, Saratoga Springs, New York, NY 12866, USA*

Received 22 August 2017; revised 9 February 2018; accepted 14 February 2018; published online 1 March 2018.
*For correspondence (e-mail mary.tierney@uvm.edu).
†Present address:Institute of Molecular, Cell and Systems Biology, University of Glasgow, Glasgow, G12 8QQ, Scotland, UK.

SUMMARY

The large retromer complex participates in diverse endosomal trafficking pathways and is essential for plant developmental programs, including cell polarity, programmed cell death and shoot gravitropism in Arabidopsis. Here we demonstrate that an evolutionarily conserved VPS26 protein (VPS26C; At1G48550) functions in a complex with VPS35A and VPS29 necessary for root hair growth in Arabidopsis. Bimolecular fluorescence complementation showed that VPS26C forms a complex with VPS35A in the presence of VPS29, and this is supported by genetic studies showing that *vps29* and *vps35a* mutants exhibit altered root hair growth. Genetic analysis also demonstrated an interaction between a *VPS26C* trafficking pathway and one involving the SNARE *VTI13*. Phylogenetic analysis indicates that *VPS26C*, with the notable exception of grasses, has been maintained in the genomes of most major plant clades since its evolution at the base of eukaryotes. To test the model that *VPS26C* orthologs in animal and plant species share a conserved function, we generated transgenic lines expressing GFP fused with the *VPS26C* human ortholog (*HsDSCR3*) in a *vps26c* background. These studies illustrate that *GFP-HsDSCR3* is able to complement the *vps26c* root hair phenotype in Arabidopsis, indicating a deep conservation of cellular function for this large retromer subunit across plant and animal kingdoms.

Keywords: retromer, *VPS26*, root hair, cell wall, *VTI13*, SNARE, growth, *Arabidopsis thaliana*.

INTRODUCTION

Endosomal trafficking pathways affects many developmental processes in plants through the internalization of proteins at the plasma membrane, trafficking of cargo to the lytic and storage vacuoles, and recycling of plasma membrane components (Geldner *et al.*, 2001; Surpin *et al.*, 2003; Sanmartín *et al.*, 2007; Kleine-Vehn *et al.*, 2008a,b). The polarized growth of root hairs has been shown to depend on endosomal trafficking pathways (Ovecka *et al.*, 2005; Voigt *et al.*, 2005; Preuss *et al.*, 2006; Larson *et al.*, 2014a), and represents a powerful system to characterize cellular components that are essential for tip growth and cell wall organization in plants. The retromer complex functions in endosomal trafficking of membrane receptors from endosomes to the Golgi in yeast (Seaman *et al.*, 1997), and consists of multi-protein complexes that are broadly conserved across eukaryotes (Oliviusson *et al.*, 2006; Koumandou *et al.*, 2011). Recently, a phylogenetic analysis of *Vacuolar Protein Sorting 26* (*VPS26*) genes, encoding a member of the large retromer complex, identified a monophyletic clade of sequences including Arabidopsis *VPS26C* (At1 g48550), which represent an ancient clade that evolved prior to the divergence of animals and plants (Koumandou *et al.*, 2011). The identification of *VPS26C* orthologs in both animal and plant species within this ancient clade led us to investigate two questions: what is the function of *VPS26C* in Arabidopsis, and is the function of *VPS26C* orthologs conserved across eukaryotes?

Retromers were first characterized in yeast (Paravicini *et al.*, 1992; Horazdovsky *et al.*, 1997; Nothwehr and Hindes, 1997; Seaman *et al.*, 1997) as a complex required for transporting membrane proteins from the late endosome to the *trans*-Golgi network (TGN), and are composed of a large cargo-binding subunit consisting of VPS35, VPS29 and VPS26 proteins, and a small subunit consisting of

sorting nexin dimers (VPS5 in yeast; SNX1/2 in animals and plants). Yeast and mammalian systems encode a single *VPS35* and *VPS29* gene, while two *VPS26* paralogs have been identified as large retromer subunits in several mammalian systems (Edgar and Polak, 2000; Haft *et al.*, 2000; Kerr *et al.*, 2005). In contrast, Arabidopsis encodes three VPS35 proteins, two VPS26 proteins and three sorting nexins (Jaillais *et al.*, 2006; Oliviusson *et al.*, 2006; Pourcher *et al.*, 2010). Initial studies in yeast and mammalian systems suggested that a pentameric retromer complex composed of both the small and large subunits is required for endosomal trafficking of cargo from late endosomes to the TGN (Seaman *et al.*, 1997). However, more recent studies suggest that the large and small subunits of the retromer in both mammalian and plant systems may also function independently in regulating specific trafficking pathways (Pourcher *et al.*, 2010; Gallon and Cullen, 2015).

In Arabidopsis, genetic analysis of the role of the large retromer complex indicates that it is essential for multiple processes in plant development, including cell polarity and organ initiation (Jaillais *et al.*, 2007), immunity-associated cell death (Munch *et al.*, 2015), and oil body biogenesis and breakdown during vegetative growth (Thazar-Poulot *et al.*, 2015). Additionally, the large retromer complex, consisting of VPS26A and VPS35A, is critical for shoot gravitropism in Arabidopsis, and has been shown to share a genetic pathway with the SNARE protein VTI11 (Yano *et al.*, 2003; Hashiguchi *et al.*, 2010) that functions in anterograde membrane trafficking pathways between the TGN and the late endosome/vacuole (Zheng *et al.*, 1999).

The large retromer complex was initially proposed to traffic vacuolar sorting receptors (VSRs) from the prevacuolar compartment(s) (PVC) to the TGN (Yamazaki *et al.*, 2008; Kang *et al.*, 2012). However, recent studies indicate that VSRs in plants bind their ligands in the endoplasmic reticulum (ER) and Golgi, and are trafficked to the TGN where the bound ligands dissociate from their receptors and the free VSRs are recycled back to the Golgi (Kudla and Bock, 2016; Künzl *et al.*, 2016; Früholz and Pimpl, 2017). These data support a model in which sorting nexins, localized to the TGN, may be involved in the retrograde sorting of VSRs in plants (Robinson and Neuhaus, 2016). This is consistent with recent studies in animal systems (Kvainickas *et al.*, 2017; Simonetti *et al.*, 2017), where sorting nexin (SNX) heterodimers are responsible for the retrograde trafficking of the mannose-6-phosphate receptor from endosomal membranes to the TGN, in a process that is independent of the large retromer subunit.

The subcellular localization of the large retromer complex in plants is still controversial (for review, see Robinson and Neuhaus, 2016). VPS35 proteins have been localized to both multivesicular bodies/PVCs (Oliviusson *et al.*, 2006; Yamazaki *et al.*, 2008; Munch *et al.*, 2015), as well as an endosomal compartment that lacks VSRs (Yamazaki *et al.*, 2008). In contrast, VPS29 has been localized to the TGN along with sorting nexins (Jaillais *et al.*, 2006, 2007; Niemes *et al.*, 2010). These differences in subcellular localization may be due to the large retromer complex protein member studied (VPS35 versus VPS29), or may suggest that different versions of the large retromer complex associate with distinct membrane populations in Arabidopsis during growth.

The presence of multiple *VPS35* and *VPS26* paralogs in Arabidopsis and other eukaryotes presents the opportunity for different versions of the large retromer complex to regulate distinct endosomal trafficking pathways. In mouse, *VPS26A* and *VPS26B* are non-redundant in function as deletion of *VPS26A* results in embryonic lethality while *VPS26B* knockout mice appear normal (Kim *et al.*, 2010). In Arabidopsis, by comparison, whereas *vps26a* and *vps26b* single-mutants appear similar to wild-type in their growth habit, growth of the *vps26a vps26b* double-mutant is severely compromised (Zelazny *et al.*, 2013), suggesting that *VPS26A* and *VPS26B* may share some redundancy in function. Nonetheless, genetic and cell biology approaches have identified several unique functions for *VPS26* and *VPS35* paralogs in Arabidopsis. For example, VPS35A and VPS29 were found to be important for trafficking of membrane proteins to the PVC (Nodzyński *et al.*, 2013), while mutations in V*PS35A* and *VPS26A* are capable of suppressing the shoot gravitropic phenotype of *vti11* mutants (Hashiguchi *et al.*, 2010). In contrast, *vps35b* and *vps26b* are defective in immunity-associated cell death and autophagy (Munch *et al.*, 2015).

In this paper, we establish that VPS26C (At1G48550) is a component of the large retromer complex in Arabidopsis and is required for root hair growth. We provide evidence for a genetic interaction between the endosomal pathways defined by the *VPS26C*-retromer complex and the SNARE *VTI13* in maintaining root hair growth. We also demonstrate that the human *VPS26C* ortholog, *HsDSCR3*, is able to complement the *vps26c* root hair growth phenotype. These results define a new member of the VPS26 family of proteins in plants, provide evidence that the *VPS26C/DSCR3* clade share

deeply conserved cellular function in eukaryotes, and establish a role for the large retromer complex in regulating root hair growth in Arabidopsis.

RESULTS

A VPS26C-VPS29-VPS35A large retromer complex is required for root hair growth

The *VPS26C* gene represents the only Arabidopsis member of an ancient gene family shared by animals and plants (Koumandou *et al.*, 2011). In order to determine its function, we examined the phenotype of two T-DNA insertion

mutants identified in the ABRC collection that were confirmed to be nulls based on quantitative reverse transcriptase-polymerase chain reaction (qRT/PCR; Figure S1). Analysis of *vps26c* root hair growth indicated that the mutant alleles were indistinguishable from wild-type seedlings when grown on Murashige–Skoog (MS) medium alone (Figure 1), but that *vps26c-1* and *vps26c-2* exhibit much shorter root hairs when grown on MS medium containing 200 mM mannitol (Figure 1a and b). Root hairs of *vps26c*-1 seedlings, expressing a *GFP-VPS26C* fusion under the transcriptional control of either the 35S promoter (Figure S2) or the *VPS26C* endogenous promoter (Figure 1a and b), were indistinguishable from those of wild-type seedlings when grown in the presence of mannitol (Figure 1a and b). Similar results were observed when *GFP-VPS26C* was expressed in the *vps26c*-2 background (Figure S2). In addition, expression of the *GFP-VPS26C* fusion under the transcriptional control of the 35S promoter did not cause any root hair growth aberrations in a wild-type background (Figure S2).

Due to the sensitivity of *vps26c* root hair growth to mannitol, we also compared root hair growth of *vps26c* with wild-type seedlings grown on MS media supplemented with 30 mM NaCl. Low concentrations of NaCl have been shown to reduce root hair growth in Arabidopsis, in part through an impact on the tip-localized Ca^{2+} gradient (Halperin *et al.*, 2003; Wang *et al.*, 2008). Root hairs of both *vps26c* mutant alleles were shorter than those of wild-type seedlings when grown on MS media supplemented with 30 mM NaCl, and this phenotype was complemented by the expression of *GFP-VPS26C* in the *vps26c* mutant background (Figure 1a and c). To confirm that this phenotype was due to sodium, we compared wild-type and *vps26c* seedlings grown on medium supplemented with 30 mM potassium chloride (Figure S3) and observed no difference in root hair length, suggesting that *vps26c* root hair growth is sensitive to sodium. These results indicate that *VPS26C* function contributes to root hair growth and that the *vps26c* root hair phenotype is sensitive to osmotic and salt stress.

The observation that *vps26c* exhibited a root hair phenotype on media supplemented with mannitol and NaCl led us to hypothesize that *VPS26C* function may be critical for polarized growth under conditions of abiotic stress. To examine this model, we performed qRT-PCR to analyze the expression of *VPS26C* in wild-type seedling roots grown on MS medium and MS medium supplemented with mannitol or NaCl (Figure 2). We found that the *VPS26C* transcript is downregulated in seedlings grown in the presence of mannitol or NaCl (Figure 2a). These data corroborate the difference in wild-type root hair length observed by Halperin *et al.* (2003) for seedlings grown on MS media supplemented with NaCl (Figure S4). We also compared this expression with that of *VSP26A* and *VPS26B* in wild-type Arabidopsis roots grown on these three media. In contrast to *VPS26C*, qRT-PCR analysis indicated that *VPS26A* and *VPS26B* transcripts were both upregulated by 200 mM mannitol, whereas only *VPS26A* showed an upregulation in the presence of 30 mM NaCl in seedling roots while *VPS26B* remained unaffected (Figure 2b and c). These results show that mannitol and NaCl selectively downregulate *VPS26C* in Arabidopsis seedling roots. Further, they show that a reduced level of the *VPS26C*, either due to the presence of mannitol or NaCl in the growth media or loss of *VPS26C* in the T-DNA insertion null mutants, negatively impacts growth of root hairs in Arabidopsis. We also used qRT-PCR to investigate whether *VPS26A* or *VPS26B* were differentially expressed in roots of *vps26c* seedlings when compared with wild-type seedling roots (Figure 2d). We found that *VPS26A* transcripts are upregulated in *vps26c* roots relative to wild-type, while *VPS26B* transcript levels were downregulated in *vps26c* (Figure 2d).

To genetically dissect the role of other large retromer complex proteins in root hair growth, we analyzed T-DNA insertion mutants for the other genes encoding the large retromer complex in Arabidopsis. Mutant alleles for each of the *VPS35* and *VPS26* family members (*VPS35A; vps35a-2, VPS35B; vps35b-3, VPS35C; vps35c-2, VPS26A; vps26a-3,* and *VPS26B; vps26b-1*) and for *VPS29* (*vps29-6*), a single copy gene in Arabidopsis, were obtained from the ABRC. qRT-PCR was used to show that each of these mutants was a null or significantly downregulated (Figure S1a, b, d–g). Mutant and wild-type seedlings were then grown for 5 days on MS medium and MS medium supplemented with 200 mM mannitol, and the length of their root hairs was compared (Figure 3). Among these mutants, only *vps35a-2*, *vps29-6* and *vps26c-1* showed a significant decrease in root hair length when compared with wild-type seedlings. Interestingly, under normal MS media conditions *vps35a-2* and *vps29-6* root hairs were also shorter than those of wild-type seedlings (Figure S5). These data provide genetic evidence indicating that VPS26C, VPS35A and VPS29 are part of a large retromer complex that functions in a pathway important for root hair growth in Arabidopsis.

We observed no other developmental phenotypes in *vps26c* mutants when compared with wild-type plants when these two genotypes were grown to seed in growth chambers. In addition, qRT-PCR analysis suggested that the *VPS26C* is expressed at comparatively similar levels in various organs throughout growth (Figure S6), a pattern consistent with existing microarray data (bar.utoronto.ca/efp/cgi-bin/efpWeb.cgi). These results suggest that while VPS26C may function in many cell types throughout plant growth, the VPS26C-large retromer complex may have a specialized role in maintaining polarized growth in root hairs.

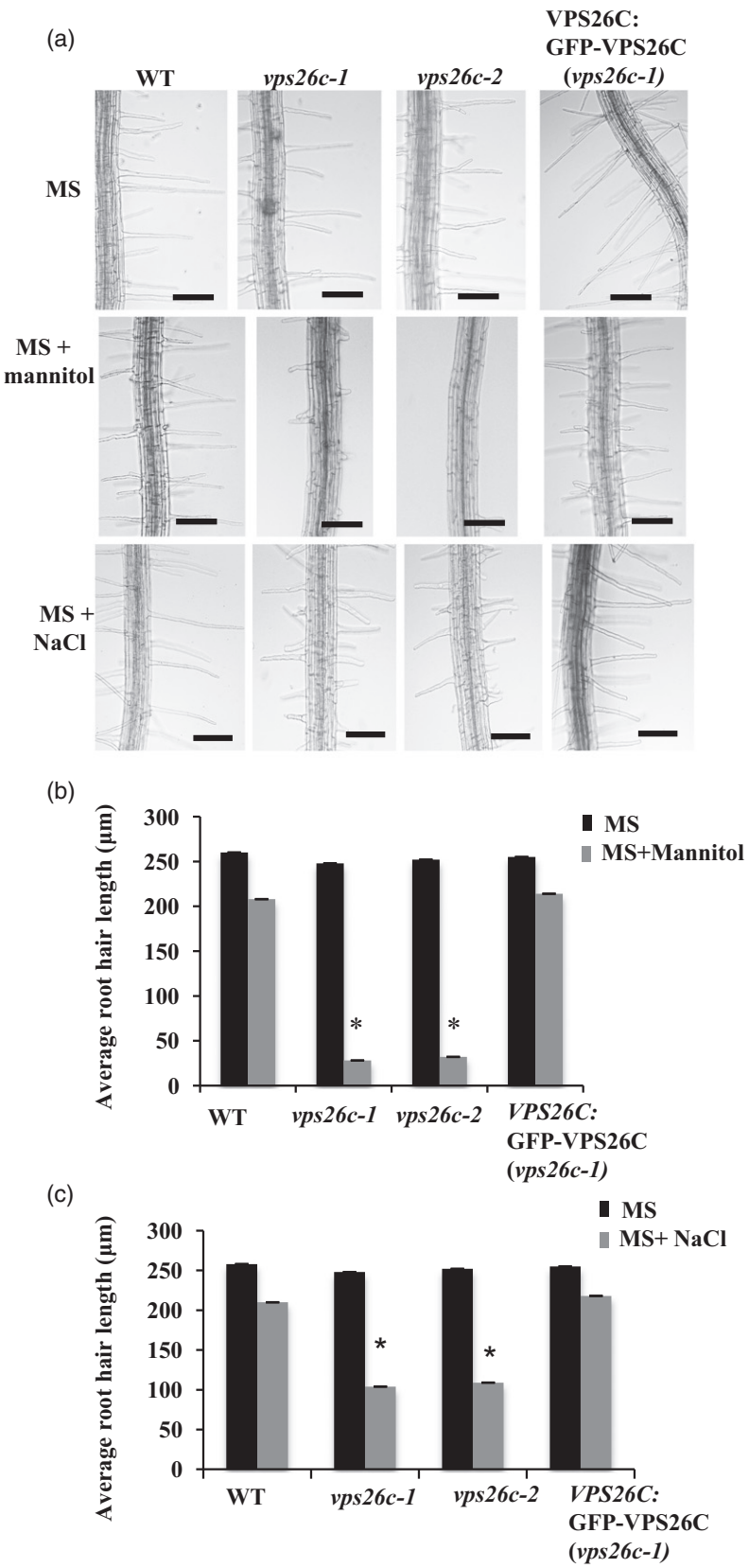

Figure 1. *vps26c* is defective in root hair growth when grown in the presence of mannitol or NaCl.
(a) Wild-type, *vps26c-1*, *vps26c-2* and *vps26c-1* seedlings expressing VPS26C:GFP-VPS26C were grown on 1 × Murashige–Skoog (MS) medium, pH 6, 1 × MS medium, pH 6 supplemented with 200 mM mannitol, and 1 × MS medium, pH 6 supplemented with 30 mM NaCl for 5 days after which root hairs were imaged using brightfield microscopy. Both *vps26c* mutants exhibited root hairs indistinguishable from wild-type when seedlings were grown on standard MS medium, but showed reduced root hair length when either mannitol or NaCl was added to the medium. The *vps26c* root hair growth phenotypes were complemented in *vps26c*-1 mutant lines expressing *VPS26C:GFP-VPS26C* for both media conditions. Three independent transgenic lines expressing *VPS26C:GFP-VPS26C* in a *vps26c-1* background exhibited similar root hair growth phenotypes. Scale bars: 100 μm.
(b) Average root hair length (μm) of 5-day-old seedlings grown on 1 × MS medium, pH 6 (black bars) and on 1 × MS medium, pH 6 supplemented with 200 mM mannitol (gray bars). Twenty seedlings per genotype per treatment were scored, and 10–15 root hairs per seedling were measured for each biological replicate. The graph shows an average of three biological replicates. Asterisks indicate statistical significance according to the Student's *t*-test, where wild-type was compared in a pair-wise manner with each of the genotypes for each treatment ($P < 0.05$). Error bars represent the standard error of the mean of three biological replicates.
(c) Average root hair length of 5-day-old seedlings grown on 1 × MS medium, pH 6 (black) and 1 × MS medium, pH 6 supplemented with 30 mM NaCl (gray). Twenty seedlings per treatment per genotype were scored, and 10–15 root hairs per seedling were measured for each biological replicate. The graph shows an average of three biological replicates. Asterisks indicate statistical significance according to the Student's *t*-test, where wild-type was compared in a pair-wise manner with each of the genotypes individually for each treatment ($P < 0.05$). Error bars represent the standard error of the mean of three biological replicates.

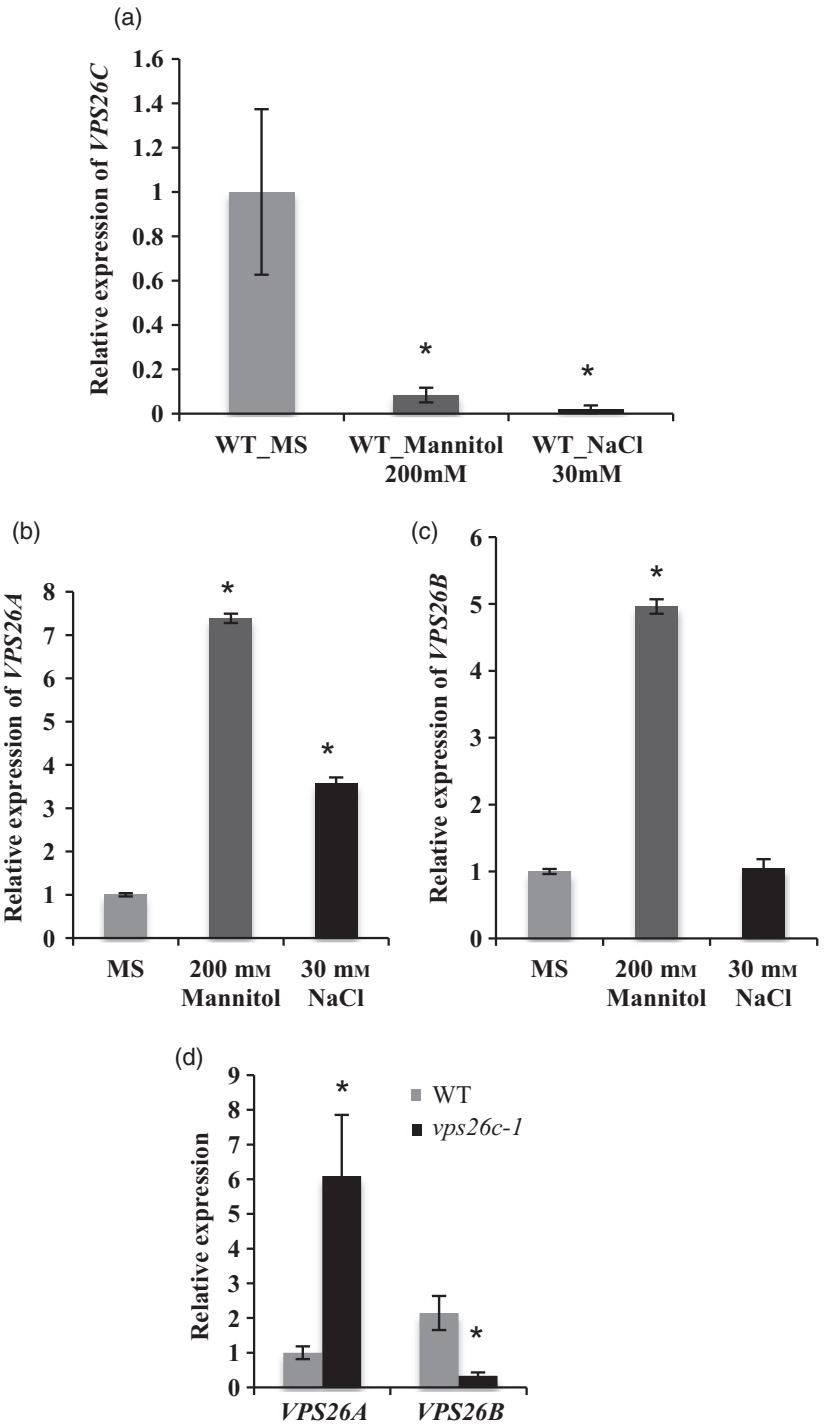

Figure 2. Differential expression of *VPS26* family members in wild-type seedlings grown under different media conditions.

(a) Quantitative reverse transcriptase-polymerase chain reaction (qRT-PCR) was used to quantitate *VPS26C* transcript levels present in roots of wild-type seedlings grown on 1 × Murashige–Skoog (MS) medium, pH 6, or 1 × MS medium, pH 6 supplemented with either 200 mM mannitol or 30 mM NaCl. Seedlings grown in the presence of either mannitol or NaCl showed a downregulation of *VPS26C* expression when compared with wild-type seedlings grown on MS alone. Asterisks indicate statistical significance according to the Student's *t*-test, where a pair-wise comparison was performed between VPS26C transcript levels from roots of seedlings grown on MS media and each of the treatments ($P < 0.05$). Error bars represent the standard error of the mean of three biological replicates, run in triplicate.

(b and c) qRT-PCR analysis of (b) *VPS26A* and (c) *VPS26B* transcript levels in roots of wild-type seedlings grown on 1 × MS medium, pH 6, or seedlings grown on 1 × MS medium, pH 6 supplemented with either 200 mM mannitol or 30 mM NaCl. In contrast to *VPS26C*, wild-type seedlings grown in the presence of either mannitol or NaCl showed an induction of *VPS26A* expression when compared with wild-type seedlings grown on MS alone. This upregulation is also observed in the expression of *VP26B* in roots of wild-type seedlings grown on media containing mannitol. Asterisks indicate statistical significance according to the Student's *t*-test, where pair-wise comparisons were performed betweenVPS26A or VPS26B transcript levels from roots of seedlings grown on MS media and the level of these same transcripts in roots of seedlings grown under each treatment condition ($P < 0.05$). Error bars represent the standard error of the mean of three biological replicates, run in triplicate.

(d) *VPS26B* in wild-type versus *vps26c* seedling roots grown on 1 × MS medium, pH 6. *VPS26A* transcript levels were induced in *vps26c* roots when compared with wild-type roots, whereas *VPS26B* transcript levels were downregulated in *vps26c* roots when compared with the wild-type roots. Asterisks indicate statistical significance according to the Student's *t*-test, where pair-wise comparisons were performed betweenVPS26A or VPS26B transcript levels from roots of wild-type seedlings grown on MS media and the level of these same transcripts in roots of *vps26c* seedlings grown on MS media ($P < 0.05$). Error bars represent the standard error of the mean of three biological replicates, run in triplicate.

VPS26C is part of the large retromer complex containing VPS35A and VPS29

The large retromer complex in eukaryotes is composed of VPS35, VPS29 and VPS26, where VPS26 and VPS35 physically interact with each other in mammalian systems (Collins *et al.*, 2008). To examine whether VPS26C associates with VPS35 as part of a large retromer complex *in planta*, we used bimolecular fluorescence complementation (BiFC), whereby *VPS26C* was used to generate a fusion with the N-terminal portion of YFP (N-YFP-VPS26C) and the three Arabidopsis *VPS35* genes were each used to create fusions with the C–terminal portion of YFP (C-YFP-

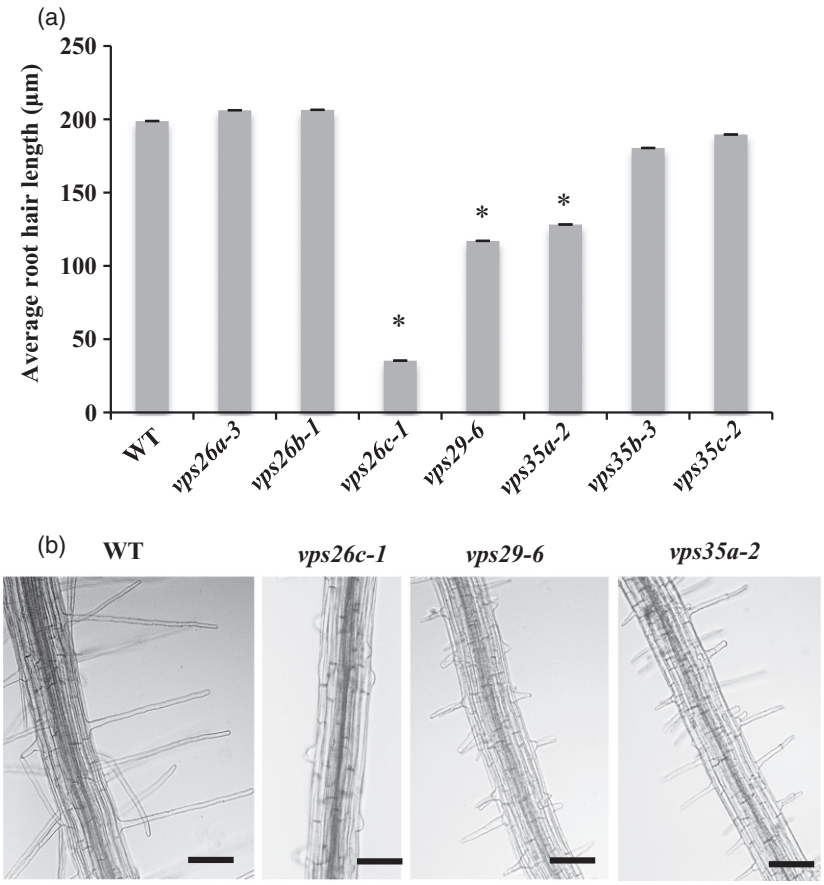

Figure 3. Large retromer complex mutants *vps35a-2*, *vps29-6* and *vps26c-1* share a defect in root hair growth.
(a) Average root hair lengths (μm) of T-DNA insertion mutants for the large retromer complex were compared with those of wild-type seedlings grown on 1 × Murashige–Skoog (MS) medium, pH 6 supplemented with 200 mM mannitol. Root hairs of 20 seedlings per treatment per genotype were scored, and 10–15 root hairs per seedling were measured for each biological replicate. The data represent the average of three biological replicates. Asterisks denote statistical significance ($P < 0.05$), determined by the Student's *t*-test, where wild-type root hair length was compared in a pair-wise manner with that for each of the retromer mutants individually. Error bars represent the standard error of mean for the three biological replicates.
(b) *vps26c-1*, *vps29-6* and *vps35a-2* and wild-type seedlings were grown on 1 × MS medium, pH 6 supplemented with 200 mM mannitol for 5 days, and were imaged using brightfield microscopy to characterize root hair growth. Root hair length of the *vps26c-1*, *vps29-6* and *vps35a-2* mutant seedlings was significantly reduced when compared with wild-type seedlings. Scale bars: 100 μm. Error bars represent the standard error of the mean for the three biological replicates.

VPS35; Figure 4). *Nicotiana benthamiana* leaves were then transfected with both an *Agrobacterium tumefaciens* strain containing a N-YFP-VPS26C construct and an *A. tumefaciens* strain containing a plasmid in which a VPS35 gene family member was fused to the C-terminal portion of YFP (C-YFP-VPS35). Using this assay, we showed that VPS26C interacted in a BiFC complex exclusively with VPS35A (Figure 4b). No evidence for a large retromer complex was observed between VPS26C and either VPS35B or VPS35C (Figure 4c and d). In addition, as was seen by Zelazny *et al.* (2013) and Munch *et al.* (2015), a positive BiFC interaction between VPS26 and VPS35 required the simultaneous expression of VPS29 in this assay (Figure 4e). We also observed a positive BiFC interaction between VPS26A and VPS35A that depended on the co-expression of VPS29-mCherry (Figure 4a), as has previously been reported by Zelazny *et al.* (2013). These results demonstrate that VPS26C colocalizes with VPS35A in the presence of VPS29 *in planta* as a large retromer complex and corroborate our genetic studies described above, predicting that VPS26C, VPS29 and VPS35A form a large retromer complex required for root hair growth in Arabidopsis.

Confocal analysis of Arabidopsis seedlings expressing VPS26C:GFP-VPS26C in a *vps26c* background indicated that VPS26C localizes, at least in part, to a membrane compartment in Arabidopsis roots (Figure 5a and b). We used Brefeldin A (BFA) sensitivity as an assay to investigate whether VPS26C may be localized to the TGN, as Niemes *et al.* (2010) have localized VPS29 to both the TGN and the core of a BFA-sensitive compartment. BFA has been shown to inhibit GTP exchange factors (Peyroche *et al.*, 1999; Richter *et al.*, 2007, 2011), and disrupts trafficking pathways between the ER and Golgi as well as endocytosis from the plasma membrane to the TGN. Five-day-old seedlings expressing GFP-VPS26C in a *vps26c* background were incubated in either vehicle alone or 100 μM BFA diluted in 1 × MS media for 90 min (Figure 5a). As a positive control, transgenic seedlings expressing the TGN marker VTI12-YFP were also incubated in vehicle alone or 100 μM BFA diluted in MS media for 90 min (Figure 5a). While VTI12-YFP formed 'BFA bodies' when incubated in the presence of BFA, VPS26C exhibited no sensitivity to BFA, as its cellular distribution appeared similar in both BFA-treated and control seedlings (Figure 5a). These data indicate that VPS26C is not localized to a BFA-sensitive compartment in Arabidopsis roots.

The large retromer subunit VPS35A has been shown to localize to late endosomal membranes and physically

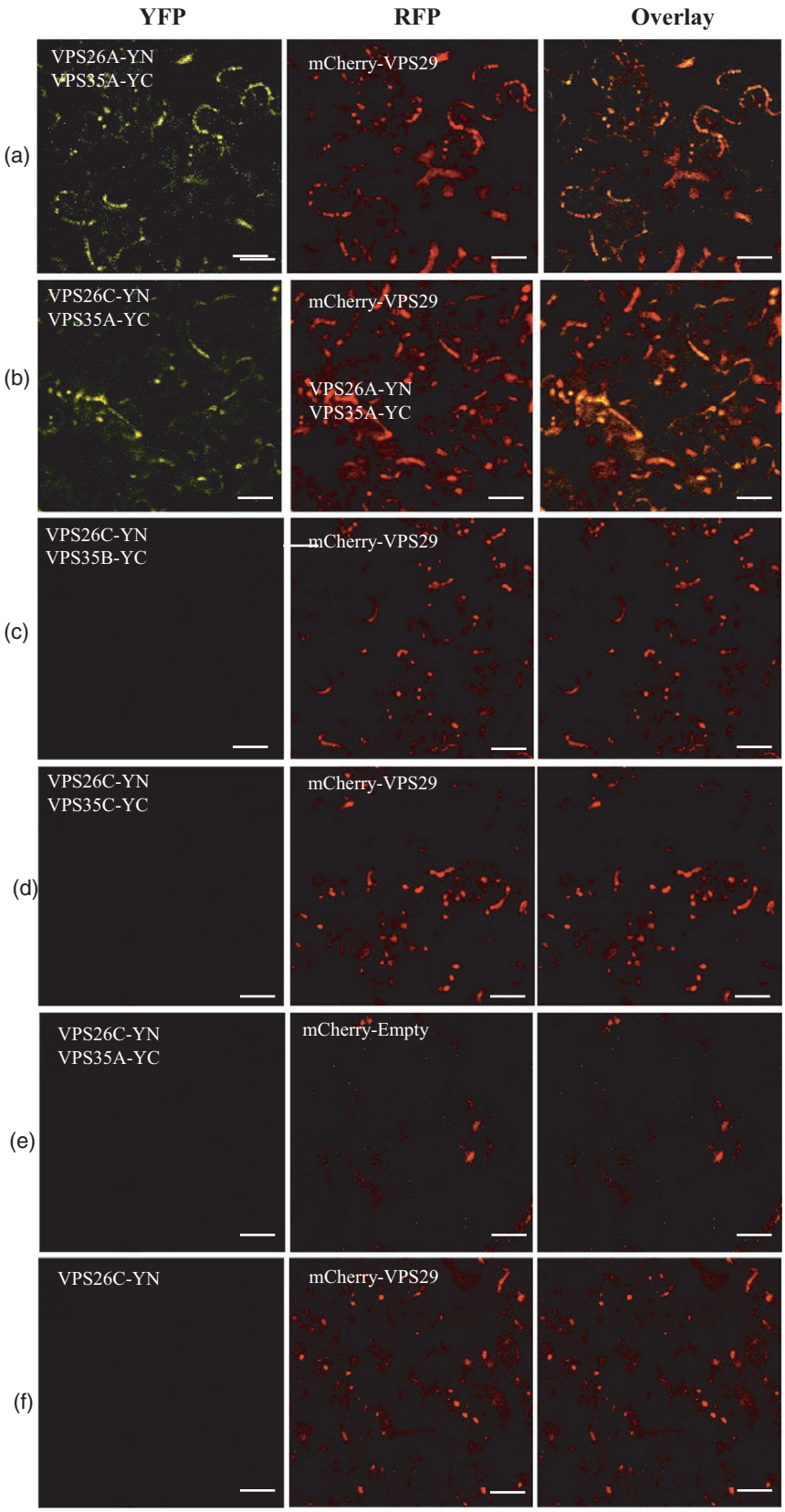

Figure 4. VPS26C forms a complex with the core retromer component VPS35 in a VPS29 dependent manner.

VPS26C-YN was co-transfected with mCherry-VPS29 and individually with each of the VPS35-YC constructs, using *Agrobacterium tumefaciens*, strain GV2260 into fully expanded 3-week-old *Nicotiana benthamiana* leaves. As a positive control, VPS26A-YN was shown to interact with VPS35A-YC, demonstrating the effectiveness of this approach (a). Bimolecular fluorescent complementation (BiFC) was used to demonstrate the formation of an *in planta* complex between VPS26C-YN and VPS35A-YC, detected by the presence of YFP fluorescence (b). This complex also co-localized with mCherry-VPS29 (a and b). No fluorescent signal was detected for either VPS35B-YC or VPS35C-YC when co-expressed with VPS26C-YN and mCherry-VPS29 in *N. benthamiana* leaves (c and d, respectively). In addition, no fluorescent signal was detected when VPS29 was not co-expressed in the cells containing VPS26C-YN and VPS35A-YC fusions (e). Lastly, when only VPS26C-YN was co-expressed with mCherry-VPS29 (f), no fluorescent signal was detected. YC, C-terminal end of YFP; YN, N-terminal end of YFP. Scale bars: 10 μm.

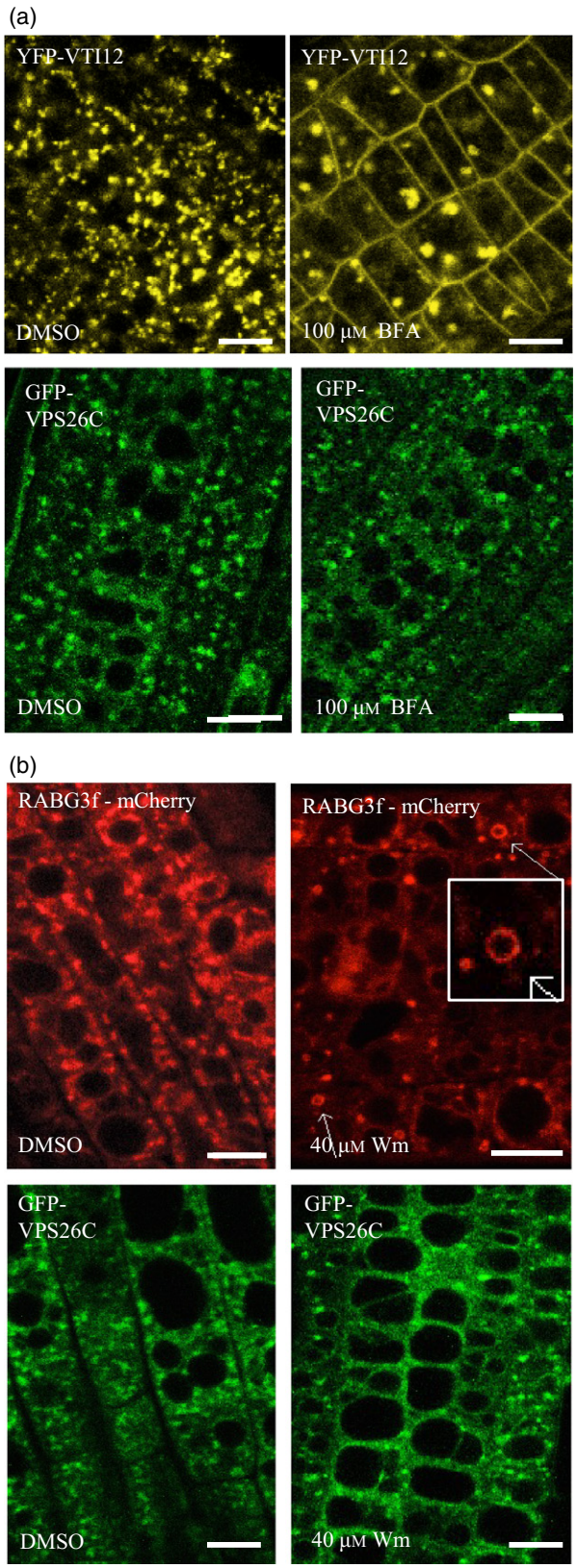

Figure 5. VPS26C localizes to membrane compartments in Arabidopsis roots that are insensitive to both Brefeldin A (BFA) and wortmannin.
(a) To determine if GFP-VPS26C localized to the *trans*-Golgi network (TGN), we treated both the transgenic seedlings expressing the TGN marker VTI12-YFP and transgenic lines expressing GFP-VPS26C with 100 μM BFA for 90 min. VTI12-YFP was sensitive to BFA, forming 'BFA-bodies' in response to this treatment, while GFP-VPS26C showed no sensitivity to BFA. Scale bars: 10 μm.
(b) To determine whether GFP-VPS26C localized to late endosomes, we treated transgenic seedlings expressing the late endosome marker RABG3f-mCherry and seedlings expressing GFP-VPS26C with 40 μM wortmannin for 90 min. While RABG3f showed sensitivity to wortmannin by forming dilated, donut-shaped structures (highlighted in the inset), the localization pattern of GFP-VPS26C was unaffected by wortmannin treatment. Scale bars: 10 μm.

interact with RABG3f, a Rab7 homolog sensitive to wortmannin (Zelazny *et al.*, 2013; Singh *et al.*, 2014). Wortmannin targets both PI3K and PI4K at concentrations higher than 1 μM, and causes swelling and fusion of late endosomal membranes in Arabidopsis roots (Jaillais *et al.*, 2008; Niemes *et al.*, 2010; Takac *et al.*, 2012). Therefore, to investigate whether VPS26C is associated with a late endomembrane compartment, we examined the sensitivity of GFP-VPS26C localization to wortmannin in Arabidopsis roots (Figure 5). Five-day-old seedlings expressing GFP-VPS26C in a *vps26c* background were incubated in either vehicle alone or 40 μM wortmannin, diluted in 1 × MS media for 90 min (Figure 5b). As a positive control, transgenic seedlings expressing RABG3f-mCherry were also incubated in vehicle alone or 40 μM wortmannin diluted in MS media for 90 min (Figure 5b). While RABG3f exhibited sensitivity to wortmannin treatment by swelling of endosomal vesicles, and forming 'donut-shaped' structures, VPS26C cellular organization was unaffected. These data suggest that the membrane compartments associated with VPS26C are distinct from endosomal compartments sensitive to wortmannin in Arabidopsis roots.

The large retromer complex subunit VPS26C and SNARE VTI13 are part of a shared endosomal trafficking pathway important for tip growth in Arabidopsis

Three members of the VTI family of SNARES in Arabidopsis have been characterized. VTI11 and VTI12 function in endosomal pathways important for trafficking cargo towards the lytic and storage vacuole, respectively (Surpin *et al.*, 2003; Sanmartín *et al.*, 2007), and VTI13 is required for root hair growth and localizes to the early endosome and vacuole membrane (Larson *et al.*, 2014a). Previous genetic studies using a suppressor screen of the *vti11* shoot gravitropic phenotype resulted in the identification of mutations in *VPS26A* and *VPS35A* (Hashiguchi *et al.*, 2010), indicating a genetic interaction between a VPS26A/VPS29/VPS35A retromer-dependent pathway and a VTI11

anterograde pathway trafficking cargo to the lytic vacuole. These studies prompted us to investigate whether VTI13 and VPS26C, both required for root hair growth, also function in a shared endosomal trafficking pathway. To address this, we generated a *vti13 vps26c* double-mutant and compared root hair growth of *vti13 vps26c* with the single-mutants and wild-type seedlings. We found that both *vti13* and *vps26c* exhibited significantly shorter root hairs than wild-type seedlings when grown in the presence of 200 mM mannitol, and these phenotypes were partially suppressed in the *vti13 vps26c* double-mutant (Figure 6). These results provide genetic evidence for a shared trafficking pathway involving the SNARE VTI13 and retromer component VPS26C that contributes to root hair growth in Arabidopsis. In addition, our results suggest that the VTI family of SNAREs may function in endosomal trafficking pathways in conjunction with the large retromer complex to control various aspects of plant development.

The observation that *vps26c* is defective in root hair growth and shares a genetic interaction with *VTI13* led us to investigate whether VPS26C function might also be essential for cell wall organization in roots of Arabidopsis. We have previously shown that in contrast to wild-type seedlings, root epidermal and hair cells of *vti13* mutants exhibit no surface labeling with LM15, a monoclonal antibody that recognizes a xyloglucan epitope in the cell wall (Larson *et al.*, 2014a). To explore this question, we used live tissue labeling (Larson *et al.*, 2014b) and confocal microscopy to probe xyloglucan organization on the surface of root epidermal cells and root hairs in *vps26c* mutants and the *vti13 vps26c* double-mutant. Interestingly, when the *vps26c* mutation was introduced into a *vti13* background, root epidermal cells and root hairs were labeled with LM15, unlike the *vti13* mutant alone (Figure 7). The suppression of the *vti13* phenotype with respect to root hair growth and cell wall organization in the *vti13 vps26c* double-mutant provides additional data to reinforce a model in which VPS26C and VTI13 contribute to a shared endosomal pathway regulating root hair growth and wall organization.

VPS26C orthologs show deep functional conservation in plants and animals

In Arabidopsis, VPS26A and VPS26B share 91% identity at the amino-acid sequence level (Figure S7), function redundantly in many aspects of plant development (Zelazny *et al.*, 2013), and are part of a large clade of sequences that

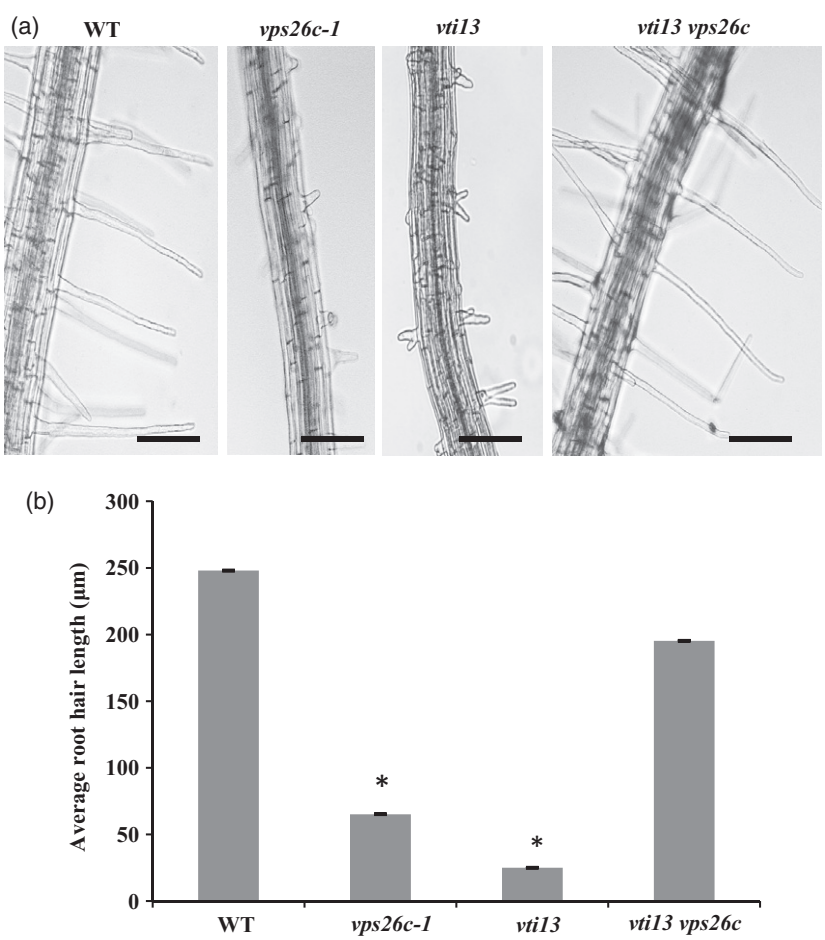

Figure 6. The *vps26c* mutant suppresses the polarized root hair growth phenotype of *vti13*.
(a) Wild-type, *vps26c-1*, *vti13* and *vti13 vps26c* double-mutant seedlings were grown on 1 × Murashige–Skoog (MS) media, pH 6 supplemented with 200 mM mannitol for 5 days and imaged using brightfield microscopy. Root hairs of the *vti13 vps26c* double-mutant were longer than either *vti13* or *vps26c*, indicating a suppression of the polarized growth defect of *vti13* in the double-mutant. Scale bars: 100 μm.
(b) Root hair lengths of wild-type, *vps26c*, *vti13* and *vti13 vps26c* mutants grown for 5 days on 1 × MS medium supplemented with 200 mM mannitol. *vps26c* and *vti13* show a reduction in root hair length, whereas root hair length of the *vti13 vps26c* double-mutant is not significantly different from wild-type. Root hairs of 20 seedlings per genotype were scored, and 10–15 root hairs per seedling were measured for each biological replicate. An average of three biological replicates is displayed above. Asterisks indicate statistical significance ($P < 0.05$), determined by the Student's *t*-test, where wild-type was compared in a pair-wise manner with each of the mutant genotypes individually. Error bars represent the standard error of the mean for the three biological replicates.

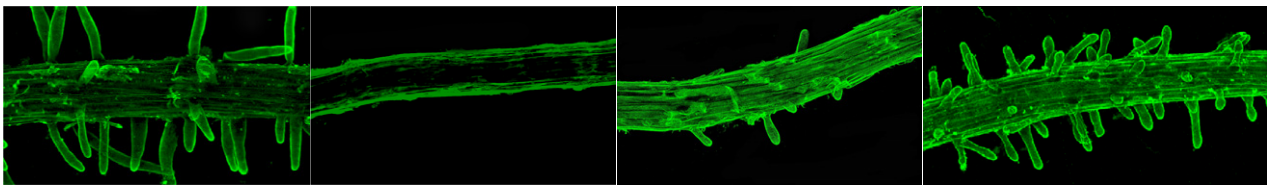

Figure 7. Cell wall organization of xyloglucan in roots of *vps26c* and the *vti13 vps26c* double-mutant is distinct from that of *vti13*.
Wild-type, *vps26c-1*, *vti13* and *vti13 vps26c* seedlings were grown on 1 × Murashige–Skoog (MS) medium, pH 6 for 5 days and labeled with LM15, a monoclonal antibody that recognizes a xyloglucan epitope in cell walls. Root epidermal cells and root hairs of wild-type and *vps26c* seedlings label similarly with LM15, whereas *vti13* root epidermal cells and root hairs do not exhibit significant LM15 labeling (as previously described in Larson *et al.*, 2014a,b). LM15 labeling of xyloglucan in root epidermal cells and root hairs is restored in the *vti13 vps26c* double-mutant, indicating that the *vps26c* mutation can suppress the *vti13* cell wall phenotype.

includes orthologs from plant and animal species (Koumandou *et al.*, 2011). Two genomic models are provided for *VPS26C* in Arabidopsis. To distinguish between these models and determine the predicted amino-acid sequence of VPS26C, we sequenced *VPS26C* cDNA generated using RNA isolated from the *vps26c* mutant expressing a *GFP-VPS26C* fusion as a template. This allowed us to define the genomic model used for *VPS26C* expression in Arabidopsis (Figure S7a). The cDNA sequence shows an alignment with one of the predicted mRNA sequences in NCBI, with accession number NM_103751.3, predicting a protein of 327 amino acids. When the predicted VPS26C amino-acid sequence is compared with that of ATVPS26A and ATVPS26B, it was found that VPS26C shares only 20 and 22% amino-acid identity with VPS26A and VPS26B, respectively (Figure S7b). This divergence in amino-acid sequence between the *VPS26* family members in Arabidopsis is also reflected by a recent phylogenetic analysis of *VPS26* orthologs in eukaryotes (Koumandou *et al.*, 2011) that indicates *VPS26C* is present in a separate clade from *VPS26A* and *VPS26B*. Moreover, the phylogenetic analysis of Koumandou *et al.* (2011) supports an ancient duplication event within the *VPS26* gene family prior to the diversification of plants and animals, giving rise to two eukaryotic lineages, the *VPS26A/B* clade and the *VPS26C/DSCR3* clade.

To examine the diversity of plant orthologs specifically within the *VPS26C/DSCR3* clade, we queried plant genome and transcriptome databases and generated a phylogenetic tree based on predicted amino-acid sequences. These analyses identified a single *VPS26C* ortholog in *Amborella trichopoda*, a species sister to other extant angiosperms, as well as in many eudicots (Figure 8). Surprisingly, unlike *VPS26A* and *VPS26B* genes (Koumandou *et al.*, 2011), *VPS26C* sequences were not identified from any of the grass genomes examined. Based on copy number and the amino-acid tree topology, our data support the loss of *VPS26C* specifically in the lineage leading to monocots, or at least within the grass clade of monocots.

To examine the sequence conservation of VPS26C/DSCR3 orthologs, we compared the amino-acid sequence of VPS26C from Arabidopsis with that predicted for the DSCR3 protein from humans (HsDSCR3; Figure 9). An alignment of these sequences indicated that the proteins are 40% identical at the amino-acid sequence level (Figure 9a). The identification of *VPS26C* orthologs in both animal and plant species led us to examine whether the function of these orthologs is conserved across eukaryotes. To this end, we transformed *vps26c-1* and *vps26c-2* with a 35S-driven GFP fusion to the human ortholog, *DSCR3*, and examined its ability to complement the Arabidopsis *vps26c* root hair growth phenotype. Comparison of root hair length between wild-type, the *vps26c* mutant and the *vps26c* mutant expressing *HsDSCR3/VPS26C* showed that expression of the human sequence is sufficient to complement the root hair growth phenotype of *vps26c* in Arabidopsis (Figures 9b and c; and S2 h). These results support a model in which the function of the human *DSCR3* ortholog is similar to *VPS26C* from plants.

DISCUSSION

VPS26C encodes a large retromer subunit essential for root hair growth

In this paper, we have characterized *VPS26C* as a new member of the *VPS26* family in Arabidopsis and have shown that loss-of-function alleles of *VPS26C* have a negative effect on root hair elongation in the presence of environmental stresses, such as mannitol or NaCl (Figure 1). BiFC analysis supported the role of VPS26C as part of a large retromer complex by showing that VPS35A was the sole member of the VPS35 protein family to form a complex with VPS26C and that this interaction required co-expression of AtVPS29 (Figure 4). The lack of interaction between VPS26C and VPS35B or VPS35C in the BiFC assay, two proteins that share significant homology with VPS35A, in addition to the positive control showing a previously characterized interaction between VPS35A and VPS26A using this assay (Zelazny *et al.*, 2013), provides strong evidence for the specificity of these interactions (Kudla and Bock, 2016). The formation of the VPS35A/

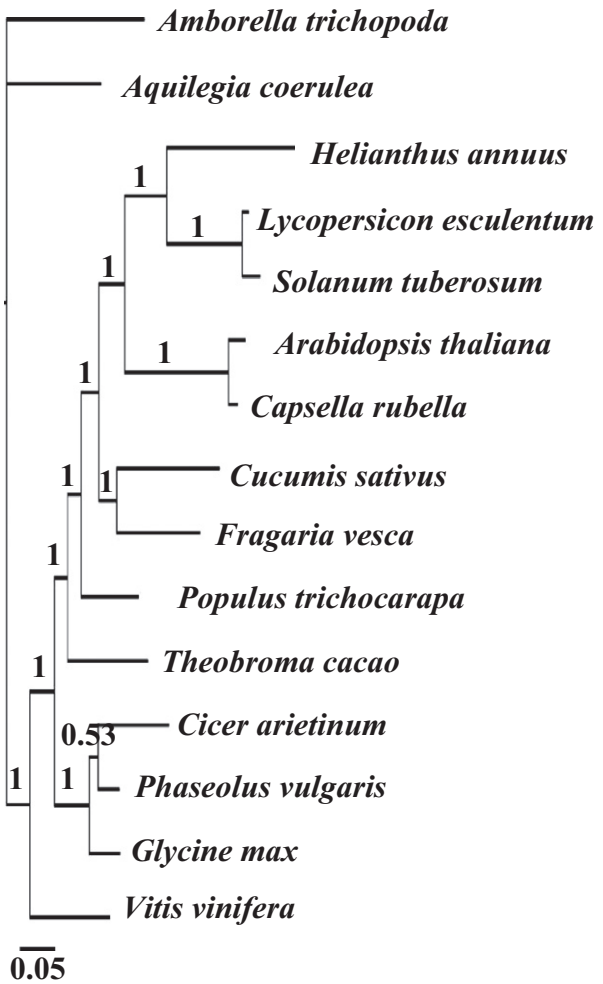

Figure 8. *VPS26C* genes are single copy in most representative angiosperms, but have likely been lost in monocots.
Fifty percent majority rule Bayesian phylogram of angiosperm *VPS26C*-like genes. Bayesian posterior probabilities are given on each interior branch. Branch lengths are in substitutions; the scale is provided below the tree.

VPS29/VPS26C protein complex *in planta* identifies a new and distinct retromer complex functioning in plant systems.

An examination of T-DNA insertion mutants for the known retromer subunits in Arabidopsis showed only *vps26c*, *vps35a* and *vps29* exhibited a root hair growth defect (Figure 3). The root hair phenotype of *vps26c* was the most severe in this assay. For VPS29, the milder root hair growth phenotype is likely due to our use of a *vps29* allele that is slightly leaky (Figure S1), while the less severe phenotype of *vps35a* may be due to the ability of VPS35B or VPS35C to substitute in part for VPS35A function *in vivo*. In contrast, the severe phenotype of *vps26C* in these studies may be due to the inability of VPS26A or VPS26B to compensate for the loss of VPS26C in regulating root hair growth (Figure 1). While VPS26A transcripts are upregulated in the *vps26c* mutant (Figure 2), the amino-acid sequence similarity between these two proteins is relatively low (Figure S7), suggesting that they may not have redundant functions.

While the genetic analysis of *vps26c* alleles in Arabidopsis initially suggested to us that a VPS26C-large retromer complex functions in endosomal trafficking pathways in response to abiotic stress, the downregulation of *VPS26C* expression in roots of seedlings grown on media supplemented with mannitol and NaCl indicates that VPS26C-retromer function may be coordinated with other cellular mechanisms required for root hair growth. Halperin *et al.* (2003) have shown that treatment of root hairs with low concentrations of NaCl also reduces root hair growth in Arabidopsis through a disruption of a tip-localized Ca^{2+} gradient. While we confirmed that root hair growth in wild-type seedlings was affected by low concentrations of NaCl under our growth conditions (Figure S4), *vps26c* exhibited even shorter root hairs, and both the mannitol and Na-induced phenotypes were complemented by a GFP-VPS26C fusion. The sensitivity of *vps26c* mutant root hairs to osmotic and salt stress suggests that the large retromer complex [VPS26C/VPS29/VPS35A] may function in a coupled manner with other cellular pathways required for root hair growth in Arabidopsis.

VPS26C functions in a cellular pathway that interacts with SNARE VTI13

A small gene family in Arabidopsis encoding the VTI-SNARES functions in distinct processes during plant growth. VTI11 is essential for shoot gravitropism (Yano *et al.*, 2003), and loss-of-function mutations in retromer subunits *VPS35A* and *VPS26A* are able to suppress the *vti11* shoot agravitropic phenotype (Hashiguchi *et al.*, 2010). We have previously shown that VTI13 is essential for root hair growth and root epidermal cell wall organization in Arabidopsis (Larson *et al.*, 2014a). Here, we show that the *vti13 vps26c* double-mutant partially suppresses the root hair growth defect that is exhibited by each of the single-mutants (Figure 6). This result indicates a genetic interaction between *VTI13*- and *VPS26C*-dependent pathways. These data also support a model in which trafficking pathways to the lytic vacuole that involve the SNARES *VTI11* and *VTI13* are coordinated with the function of distinct VPS26-large retromer complexes.

While a cellular mechanism to explain these genetic interactions has not yet been determined for either *VTI11* or *VTI13*, several possibilities exist. It is possible that mutations in large retromer subunits enhance the ability of other VTI-family members to substitute for VTI13 function in root hair growth. This model has been put forward for the genetic interaction between *VTI11* and a large retromer complex containing *VPS26A* and *VPS35A* (Hashiguchi *et al.*, 2010). We have shown that *VPS26A* transcript is

(a)

```
Arabidopsis     MATATTVNVKLSRSNRIYRSSEPVEGKIVIKSATSISHQAIRLSVNGSVNLQVRGGSAGV   60
Human           --MGTALDIKIKRANKVYHAGEVLSGVVVISSKDSVQHQGVSLTMEGTVNLQLSAKSVGV   58
                   .*::::*:.*:*:::*::.* :.* :**.*  *:.**.: *:::*:****: . *.**

Arabidopsis     IESFYGVIKPIQIVKKTIEVKSSGKIPPGTTEIPFSLNLREPGEGIVEKFYETFHGTNIN   120
Human           FEAFYNSVKPIQIINSTIEMVKPGKFPSGKTEIPFEFPLHLKGNK---VLYETYHGVFVN   115
                :*:**. :*****::.***: . **:* *.*****.: *:  *:     :***:**. :*

Arabidopsis     IQYLLTADIPRGYLHKPLSATMEFIIESGRVDLPERPIPPEIVIFYI-TQDTQRHPLLPD   179
Human           IQYTLRCDMKRSLLAKDLTKTCEFIVHSAPQKGKFTPSPVDFTITPETLQNVKERALLPK   175
                *** * .*: *. * * *: * ***:.*.  .    * * ::.*     *:.:.: ***.

Arabidopsis     IKTGGFRVTGKLATQCSLQDPLSGELTVEASSVPITSIDIHLLRVESIIVGERIVTETSL   239
Human           FLLRG----HLNSTNCVITQPLTGELVVESSEAAIRSVELQLVRVETCGCAEGYARDATE   231
                :   *       :*:* : :**:***.**:*.. * *::::*:***:   .*  . :::

Arabidopsis     IQSTQIADGDVCRNMTLPIYVLLPRLLMCPSVFAGPFSVEFKVCITISFKSKLAKAQPKS   299
Human           IQNIQIADGDVCRGLSVPIYMVFPRLFTCPTLETTNFKVEFEVNIVVLLHPDHL------   285
                **. *********.:::***:::***: **:: :  *.***:* *.: :: .

Arabidopsis     DPTAPRLWMALERLPLELVRTKRDQFSC   327
Human           ---------ITENFPLKLCRI-------   297
                         *.:**:* *
```

(b)

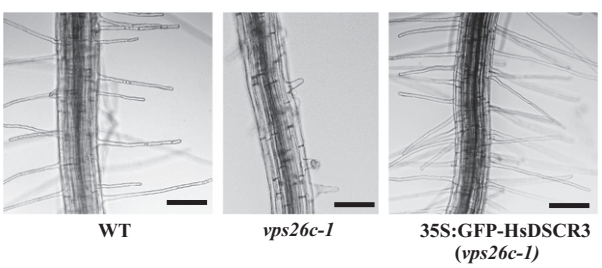

(c)

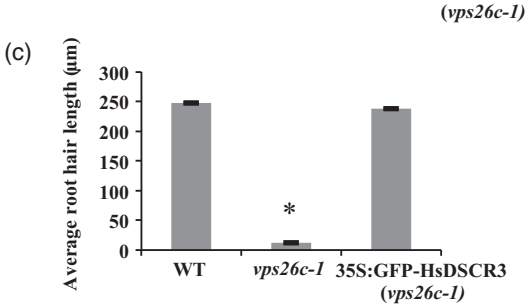

Figure 9. *AtVPS26C* and *HsDSCR3* orthologs share 40% amino-acid identity and a conserved function in Arabidopsis.
(a) Alignment of ATVPS26C and HSDSCR3 illustrates that these orthologs share 40% amino-acid sequence identity. Legend: (*): fully conserved residues; (:) conserved residues with strongly similar properties; (.) conserved residues having less similar properties.
(b and c) Wild-type, *vps26c-1* and *vps26c-1* seedlings expressing *35S:GFP-HsDSCR3* were grown on Murashige–Skoog (MS) media, pH 6 supplemented with 200 mM mannitol for 5 days, after which root hair growth was imaged using brightfield microscopy. Fifteen seedlings per genotype were scored and 10–15 root hairs per seedling were measured for each biological replicate. The graph represents the average of three biological replicates. Three independent transgenic lines expressing *GFP-HsDSCR3* in the *vps26c* mutant background were examined. Asterisks denote statistical significance ($P < 0.05$), according to Student's *t*-test, where wild-type root hair length was compared in a pair-wise manner with root hair length of *vps26c-1* and *vps26c-1* seedlings complemented with GFP-HsDSCR3 individually. Error bars represent the standard error of the mean for the three biological replicates.

upregulated in roots of *vps26c*, suggesting that *VPS26A* may function to partially suppress the root hair phenotype in the *vti13 vps26c* double-mutant. However, other potential mechanisms need to be considered. The large retromer complex protein *VPS35A* regulates trafficking of cargo to the lytic vacuole (Nodzyński *et al.*, 2013), and *VPS35B* function is required for normal function of late endocytic compartments in plants (Munch *et al.*, 2015). Thus, large retromer complex function may be required for both anterograde and retrograde trafficking pathways between the lytic vacuole and the TGN.

We had previously shown that epidermal cell wall organization of *vti13* root epidermal cells and hairs is defective in xyloglucan organization (Larson *et al.*, 2014a). Interestingly, we found that when a *vps26c* mutation is introduced into the *vti13* background, xyloglucan staining is indistinguishable from that of wild-type (Figure 7). The observation that xyloglucan can be detected in roots of the *vti13 vps26c* double-mutant indicates that the defect in *vti13* wall organization is not due to defects in xyloglucan synthesis. While future experiments will be needed to define a cellular mechanism responsible for the *vti13* and *vps26c* root hair phenotypes, these data support a model in which the *vps26c* mutant can suppress both the *vti13* root hair growth phenotype and xyloglucan organization phenotype within the *vti13 vps26c* double-mutant.

VPS26C associates with endosomal membranes insensitive to BFA and wortmannin

VPS35A has been localized to the prevacuolar membrane and is required for the trafficking of membrane proteins in plants (Nodzyński *et al.*, 2013), while VPS35B has been localized to a wortmannin-sensitive, late endosomal compartment in Arabidopsis (Munch *et al.*, 2015). In addition, proteomic studies have localized VPS35A and VPS35B to a RABG3f-enriched compartment (Zelazny *et al.*, 2013; Heard *et al.*, 2015), consistent with their presence on late endosomal membranes. In contrast, Niemes *et al.* (2010) have

localized VPS29 to the TGN in Arabidopsis, while Jaillais *et al.* (2007) found VPS29 to localize to a wortmannin-sensitive compartment together with SNX1 and RABF2b. To investigate the nature of the membrane compartment associated with VPS26C in roots, we contrasted the cellular distribution of GFP-VPS26C and VTI12-YFP in control seedlings and seedlings treated with BFA. We also compared control seedlings and seedlings expressing GFP-VPS26C or RABG3f-mCherry treated with wortmannin (Figure 5a and b). These studies showed that while VTI12-YFP, a TGN marker (Sanderfoot *et al.*, 2001), was sensitive to BFA and RABG3f-mCherry, a late endosomal marker (Singh *et al.*, 2014), was sensitive to wortmannin, the distribution of GFP-VPS26C on cellular membranes was unaffected by either of these compounds in root epidermal cells.

Recent analysis of the subcellular localization of VPS26C (DSCR3) in human cell culture indicates that a VPS26C/VPS29/VPS35L protein complex resides on endosomal membranes, with VPS26C directly interacting with SNX17 while the classical retromer complex in humans involves an interaction between VPS35 and the WASH complex in association with SNX27 (McNally *et al.*, 2017). These authors also demonstrated that the human complex containing VPS26C, termed the 'retriever', is responsible for recycling a distinct subset of proteins to the plasma membrane when compared with the classical retromer complex in humans (McNally *et al.*, 2017). These results open up the possibility that VPS26C in Arabidopsis may also be part of a 'retriever' complex in plants and may not share an intracellular location with previously studied large retromer complexes. Future experiments, focused on identifying membrane proteins that associate with the VPS26C/VPS29/VPS35A complex in plants, their intracellular location and the cargo that may be recycled by this complex will assist in establishing the identity of the membrane compartment associated with VPS26C, as well as define its role in endosomal trafficking pathways required for polarized growth in root hairs.

VPS6C shares a conserved cellular function across eukaryotes

Amino-acid sequence comparisons showed that while VPS26C shares low amino-acid sequence similarity with VPS26A and VPS26B in Arabidopsis (Figure S7), it shares significant similarity with DSCR3-like sequences present in both animals and plants (Koumandou *et al.*, 2011). We used phylogenetic analysis to show that a single *VPS26C* gene is found in the genomes of most land plants surveyed (Figure 8), although it appears to be absent from the genomes of monocots for which genomic data are available. This raises the interesting question of whether V*PS26A* and/or *VPS26B* can compensate for the loss of *VPS26C* in retromer-dependent pathways controlling monocot tip growth, or whether monocots utilize a different endocytic trafficking pathway to regulate root hair growth. Further experiments will be required to determine if functional orthologs of the Arabidopsis VPS26C protein exist in monocot species.

Comparison of ATVPS26C and HSDSCR3 amino-acid sequences indicated a conservation of protein sequence between these orthologs (Figure 9). Therefore, we asked whether VPS26C/DSCR3 orthologs are conserved in function across animal and plant kingdoms. We found that a *GFP-HsDSCR3* fusion was able to complement the root hair growth phenotype of *vps26c-1* and *vps26c-2*, indicating that the human ortholog can carry out all the functions of *VPS26C* needed for root hair growth (Figure 9).

The ability of HsDSCR3 to complement the *vps26c* root hair phenotype in Arabidopsis suggests that VPS26C/DSCR3 proteins have a conserved function in eukaryotic cells. A VPS26C/HsDSCR3 complex, termed the 'retriever' has been characterized within human cells and has been shown to function in an endosomal trafficking pathway that involves the recycling of a number of membrane proteins (McNally *et al.*, 2017). A proteomic analysis of the VPS26C-retriever complex was shown to include a minimum of 10 proteins involved in ARP2/3 activation and membrane binding (McNally *et al.*, 2017). Interestingly, many of these proteins do not have homologs in plants. Thus, future studies will be necessary to identify other proteins that interact with the VPS26C/VPS35A/VPS29 complex in a cellular pathway regulating polarized growth and cell wall organization in Arabidopsis.

EXPERIMENTAL PROCEDURES

Plant material, T-DNA insertion verification and growth conditions

Analysis of wild-type and SALK mutant lines was performed using the Columbia-0 ecotype of Arabidopsis. The growth medium for Arabidopsis seedlings consisted of 1 × MS salts (Murashige and Skoog, 1962), 1% (w/v) sucrose, 5 mM 4-morpholineethanesulfonic acid sodium salt (MES), pH 6, 1 × Gamborg's vitamin solution and 1.3% (w/v) agarose (Invitrogen). For plants grown to maturity, seeds were sown on soil (Transplanting Mix, Gardener's Supply, Intervale Rd, Burlington, VT, USA) and placed in Conviron MTR30 growth chambers (Conviron, Winnipeg, CA, USA), using cool-white lights (80 μmol m^{-2} sec^{-1}; Licor photometer LI-189) under a 16:8 h light:dark cycle at 19°C.

Two *vps26c* T-DNA mutant alleles, SALK_100616 (*vps26c-1*) and SALK_036953 (*vps26c-2*), were obtained from the Arabidopsis Biological Research Center (ABRC), and polymerase chain reaction (PCR) was used to confirm the T-DNA insertion in *VPS26C* (AT1G48550; NCBI Reference sequence: NC_003070.9; Figure S8). To generate the *vti13 vps26c* double-mutant, *vps26c-1* homozygotes were crossed with *vti13* homozygotes and F2 plants were genotyped for the two mutations using PCR. Seedlings homozygous for both the *vps26c* and *vti13* T-DNA insertion alleles were grown to seed, and T3 seedlings were analyzed for root hair growth. Primer sequences used for genomic PCR are listed in Table S1.

The *vps26c-1* and *vps26c-2* mutants were transformed separately with *35S:GFP-VPS26C* and *VPS26C:GFP-VPS26C*, and

transgenic lines containing these constructs were selected for BASTA resistance. T3 homozygous lines expressing the *GFP-VPS26C* constructs were analyzed for complementation of the *vps26c* mannitol/NaCl root hair phenotype. In addition, *vps26c* mutants were transformed with the *VPS26C* human ortholog (*35S:GFP-HsDSCR3*), and seedlings from homozygous lines expressing *GFP-HsDSCR3* were analyzed for complementation of *vps26c* root hair phenotypes.

Characterization of root hair phenotypes

Seeds were sterilized using 20% (v/v) bleach, followed by five-six washes in sterile distilled water. The sterilized seeds were stored in sterile water overnight in the dark at 4°C before plating them on solid media. Seedlings were grown on MS medium using Petri plates placed vertically under continuous white light at 20°C for 5 days. Where indicated, 200 mM mannitol or 30 mM NaCl was included in the growth medium. To characterize root hair shape and growth, seedlings were mounted in sterile water on glass slides. Images were taken using a Nikon Eclipse TE200 inverted microscope with SPOT imaging software (Diagnostic Instruments). The lengths of 10–15 root hairs per seedling for at least 10 seedlings per genotype were measured, using the calibrating tool in the SPOT software, and a Student's *t*-test was used for statistical analysis.

Construction of VPS26C-GFP fusions

To generate the *35S:GFP-VPS26C* construct, *VPS26C* was amplified by PCR using genomic DNA and primers described in Table S1. The *VPS26C* PCR product was cloned into pENTR (Invitrogen) and was subsequently recombined into pB7WGF2 to create a *35S:GFP-VPS26C* fusion. This construct was transformed into *Escherichia coli*, DH5α, and subsequently into *A. tumefacians*, GV3101, and was used to transform *35S:GFP-VPS26C* into Arabidopsis using the floral dip method (Clough and Bent, 1998; Zhang *et al.*, 2006).

To generate the *GFP-HsDSCR3* fusion, cloned *HsDSCR3* cDNA was purchased from Origene Technologies (Cat. No.- RC210755) and used as a template for PCR amplification with primers described in Table S1. The *HsDSCR3* PCR product was cloned into pENTR (Invitrogen) and transformed into *E. coli*, strain DH5α. The insert was confirmed by PCR, and subsequently recombined into pB7WGF2 using Gateway technology, according to manufacturer's instructions. The *GFP-HsDSCR3* construct in pB7WGF2 was transformed into *A. tumefaciens* and then into Arabidopsis as described above.

To generate a *VPS26C:GFP-VPS26C* construct, 2 kb of genomic sequence upstream of the V*PS26C* translation start codon was amplified using primers containing a SacI and a SpeI restriction site at their respective 5′-ends (Table S1). The *VPS26C* promoter PCR product was cloned into pENTR (Invitrogen), digested with SacI and SpeI, and ligated upstream of *GFP-VPS26C* in the B7WGF2 backbone that had previously been digested with SacI and SpeI to remove the 35S promoter. The *VPS26C:GFP-VPS26C* construct was transformed into *E. coli* DH5α and subsequently into *A. tumefacians*, strain GV3101 for transformation into Arabidopsis.

RNA isolation and transcript analysis using RT-PCR and qRT-PCR

For transcript expression analysis across the developmental stages of Arabidopsis, 7-day-old seedling roots, 7-day-old whole seedlings, leaves (45-day-old plant, 10–12 leaved rosette, bolted), stems, open flowers and green siliques were collected for three biological replicates. For null mutant analysis, 7-day-old seedlings were pooled from each genotype and three biological replicates were generated for RNA extraction. For all other RT-PCR and qRT-PCR assays, 5-day-old seedling roots were used for RNA isolation. Roots from approximately 200 seedlings were pooled for each genotype and treatment, and three biological replicates were generated. Root tissue was excised from the seedlings leaving only the differentiation, elongation and meristematic regions of the root. All isolated tissues were frozen, ground in liquid nitrogen, and stored at −80°C. Total RNA was extracted using a Qiagen RNeasy Plant Mini Kit, quantified using a nanodrop (ThermoScientific) followed by generation of first-strand cDNA using Superscript II Reverse Transcriptase (Invitrogen), according to the manufacturer's instructions. For semi-quantitative RT-PCR, root cDNA was used as a template, and PCR products were amplified using Phusion polymerase (New England Biolabs) according to the manufacturer's instructions. For qRT-PCR, the first-strand cDNA was diluted 1:10 and then used as a template with iTaq Universal SYBR green Supermix (Bio-Rad). An Applied Biosystems Step-one Plus instrument was used to run the qRT-PCR. Three technical and three biological replicates were used for each qRT-PCR cycle. The differential expression values of transcripts were standardized against the transcript expression of *EF1α* and *ACT2* housekeeping genes. The sequence of primers used for RT- and qRT-PCR are described in Table S1.

BiFC analysis

Full-length genomic clones were amplified for *VPS26A*, *VPS26C*, *VPS29*, *VPS35A*, *VPS35B* and *VPS35C* using Arabidopsis seedlings. The primers used for each of the PCR reactions are listed in TableS1. *VPS26A* and *VPS26C* were each cloned into the destination vector pSAT4-DEST-nEYFP-C1 (CD3-1089, ABRC) to create N-terminal YFP fusion constructs. *VPS35A*, *VPS35B* and *VPS35C* were each cloned into destination vector pSAT5-DEST-cEYFP-C1 (CD3-1097, ABRC) to form C-terminal YFP fusion constructs. *VPS29* was amplified using primers containing KpnI and BamHI restriction enzyme sequences at their 5′-ends, and cloned into pENTR (Invitrogen). Both *VPS29* in pENTR and the destination vector pSAT6-mCherry-C1-B (CD3-1105, ABRC) were digested with KpnI and BamHI, gel purified and a mCherry-VPS29 fusion was generated using T4 DNA ligase and the pSAT6 backbone. All constructs were transformed into *E. coli* strain DH5α. The presence of VPS sequences was confirmed using PCR, followed by transformation into *A. tumefaciens*, strain GV2260 before transfecting into *N. benthamiana* leaves.

Nicotiana benthamiana leaves were co-transformed with two *A. tumefaciens* strains containing a N-terminal YFP-VPS26C fusion and a C-terminal YFP fusion to either *VPS35A*, *VPS35B* or *VPS35C* in a manner similar to that described by Munch *et al.* (2015) with the following changes. N-terminal *YFP-VPS26A* was co-transformed with a C-terminal YFP fusion to *VPS35A* as a positive control. All transformations also included an *A. tumefaciens* strain containing *VPS29* fused with *mCherry*. Overnight cultures of *A. tumefaciens* containing the various YFP fusions were grown with appropriate antibiotic selection at 28°C, pelleted and resuspended in 10 mM magnesium chloride to reach a final OD600 = 1.5. Two microliters of 100 mM acetosyringone was added per ml of resuspended bacterial culture. Bacterial suspensions were incubated at room temperature in the dark for 4 h without shaking and then infiltrated into the abaxial side of fully expanded 4-week-old *N. benthamiana* leaves (1 ml of culture per leaf). Infected plants were grown under continuous light

at 20°C for 2–3 days, after which leaf tissue was imaged using confocal microscopy.

Confocal microscopy and drug treatment

Confocal images were obtained using a Zeiss LSM 510 META confocal laser-scanning microscope. The LSM META software was used to acquire images, which were then processed using ImageJ (https://imageJ.net/Citing). The GFP-VPS26C lines were excited with a 488-nm laser, and emissions were captured using a 505–530-nm bandpass filter. The YFP protein fusions for BiFC assays were excited with a 514-nm laser, and emissions were captured using a 530–600-nm bandpass filter. The mCherry fusion in the BiFC assays was excited with an additional laser of 545 nm, and emissions were acquired using a 560–615-nm bandpass filter. All signals were captured sequentially and superimposed in a final composite image.

To investigate the sensitivity of VPS26C to BFA or wortmannin, 5-day-old seedlings were incubated in multi-well plates with either vehicle alone, or with 100 μM BFA or 40 μM wortmannin diluted in 1 × MS medium for 90 min before imaging using confocal microscopy. Excitation and emission wavelengths for YFP, GFP and mCherry fusions were as described above. VTI12-YFP (WAVE 13Y; CS781654) and RabG3f-mCherry (WAVE 5R; CS781670) were used as positive controls for the BFA and wortmannin sensitivity assays, respectively.

Immunohistochemistry of roots and root hairs of Arabidopsis

For immunofluorescence analysis of roots hairs, the protocol described in Larson *et al.* (2014b) was employed. Briefly, whole roots were washed 3 × (5 min each) in fresh MS medium, and then placed in blocking solution consisting of 1% non-fat Carnation Instant Milk in MS for 30 min with gentle agitation. After washing 3 × with MS, the roots were placed in the primary antibody label consisting of LM15 (Plant Probes, Leeds, UK) diluted 1/10 in MS for 90 min. After three washes with MS and a 30-min block (see above), the roots were then incubated in the secondary antibody label consisting of anti-rat TRITC (Sigma Chemical, St Louis, MO, USA) diluted 1/75 in MS for 90 min. The roots were then washed 3 × with MS, positioned in the well of immunoslide (EMS; Ft. Washington, PA, USA) containing 50 μl MS and then covered with a glass coverslip.

Roots were observed with an Olympus Fluoview 1200 confocal laser-scanning microscope (CLSM) using a 559 laser, and TRITC filter set with an excitation range of 515–550 nm and an emission range of 600–640 nm. Intensity levels of LM15-labeled root hair walls were adjusted using the Hi-Lo pseudocolor control of the CLSM. The captured image was then changed to green pseudocolor. Root hair images were captured at a maximum intensity under conditions that did not show any saturation signals. In these experiments, a small level of non-specific labeling was observed in root epidermal cells. All labeling was repeated 3 ×, and the control included the elimination of the primary antibody step.

Phylogenetic analysis of VPS26C sequences

For phylogenetic analyses, gene sequences of *VPS26C* from 15 angiosperm genomes were downloaded from Phytozome (v.12.1) or NCBI. Predicted VPS26C amino-acid sequences were first aligned with the program Muscle, as implemented in Geneious version 10.1 (Kearse *et al.*, 2012). The final six positions in the alignment were trimmed from five accessions to yield sequences of uniform length. To improve posterior-probability support for the phylogeny, the amino-acid alignment was reconstructed with all parameters at default values except the gap-open score, which was set to 0 to yield the maximum allowable number of gaps. All sites in the alignment with gaps (55 of 336) were removed from the dataset, because support values were further improved. The alignment from which the gaps were removed is provided in Table S2.

Phylogenetic analysis was performed using the program MrBayes 3.2.6 (Ronquist *et al.*, 2012) running on EXSEDE via the Cipres Portal (Miller *et al.*, 2010). A Markov Chain Monte Carlo analysis was performed for the amino-acid sequences with four independent Markov chains run for five million generations; trees were sampled every 1000 generations. Stationarity was determined using the log-likelihood scores for each run plotted against generation in the program Tracer version 1.5 (Rambaut and Drummond, 2007). Twenty-five percent of the trees were discarded as a burn-in phase, and a 50% majority-rule consensus tree was calculated for the remaining trees. The species sister to all remaining angiosperms (*A. trichopoda)* was used as the outgroup for the phylogenetic analyses (Stevens, 2001).

Statistical analysis

Statistical analyses were done using a Student's *t*-test, where pair-wise comparison was performed between genotypes or treatments. For example, root hair growth measurements were compared in a pair-wise fashion between wild-type and each of the mutants individually, and significance was accepted at the $P < 0.05$ level.

ACCESSION NUMBERS

The sequence and T-DNA insertion details mentioned in this publication are available at the Arabidopsis Information Resource (TAIR) and are indicated by the following accession numbers. The mutant alleles and SALK T-DNA insertion lines used for genetic studies are denoted in parentheses, respectively: *VPS26A*, AT5G53530 (*vps26a-3*, CS831947); *VPS26B*, AT4G27690 (*vps26b-1*, SALK_142592); *VPS26C*, AT1G48550 (*vps26c-1*, SALK_100616; *vps26c-2*, SALK_036953); *VPS29*, AT3G47810 (*vps29-6*, SALK_051994); *VPS35A*, AT2G17790 (*vps35a-2*, SALK_079196); *VPS35B*, AT1G75850 (*vps35b-3*, SALK_052160); *VPS35C*, AT3G51310 (*vps35c-2*, SALK_099733); *VTI13*, AT3G29100 (SALK_075261).

ACKNOWLEDGEMENTS

Jordan Humble identified the root hair phenotype of *vps26c* alleles in response to mannitol. Emily Larson generated the *VPS26C:GFP-VPS26C* construct and performed crosses to generate the *vti13 vps26c* double-mutant. David Barrington generated a phylogenetic tree for *VPS26C* orthologs in plants. David Domozych performed the immunohistochemistry using LM15 monoclonal antibodies to characterize the distribution of xyloglucans on the surface of epidermal cells in wild-type, *vti13*, *vps26c* and *vti13 vps26c* seedling roots. Suryatapa Ghosh Jha analyzed the *vps26c* alleles for their response to mannitol and NaCl in the media and other retromer mutant phenotypes, generated complemented lines for both *vps26c-1* and *vps26c-2*, performed BiFC analysis of VPS26C *in planta*, confocal microscopy analysis, qRT/PCR analysis of *VPS26C* expression during plant growth, and cloned and

complemented the *vps26c* alleles with the *VPS26C/DSCR3* human ortholog. Suryatapa Ghosh Jha wrote the first draft of the manuscript; Mary Tierney edited the manuscript and supervised the research. The authors have no conflicts of interest to declare. The authors thank Jeanne Harris, Jill Preston and Georgia Drakakaki for insightful comments and suggestions on the manuscript. The authors also thank Georgia Drakakaki for providing them seeds of the VTI12-YFP (Wave 13Y) line. Imaging work was done at the Microscope Imaging Facility at the University of Vermont. Confocal microscopy was performed on a Zeiss 510 META laser-scanning confocal microscope supported by NIH Award Number 1S10RR019246 from the National Center for Research Resources. USDA-Hatch Grants VT-H02001 and VT-H02311 and funds from the Department of Plant Biology, University of Vermont, supported this research.

SUPPORTING INFORMATION

Additional Supporting Information may be found in the online version of this article.

Figure S1. T-DNA mutant lines of retromer subunits exhibited strongly reduced gene expression.

Figure S2. Overexpression of VPS26C does not affect root hair growth in wild-type seedlings, and VPS26C/DSCR3 GFP-fusions complement the *vps26-2* root hair phenotype.

Figure S3. Root hair length is unaffected when seedlings are grown in MS media supplemented with KCl.

Figure S4. Supplementation of MS media with mannitol and NaCl results in a reduction in root hair length in wild-type seedlings.

Figure S5. *vps35a* and *vps29* exhibit shorter root hairs than wild-type seedlings independent of media conditions.

Figure S6. qRT/PCR analysis of VPS26C expression in *Arabidopsis thaliana*.

Figure S7. Genomic model for *VPS26C* and alignment of VPS26C with gene family members VPS26A and VPS26B.

Figure S8. Genotyping of WT, *vps26c-1* and *vps26c-2* expressing the GFP-VPS26C/DSCR3 fusions using gene-specific primers and genomic PCR.

Table S1. List of primers

Table S2. Alignment of VPS26C sequences used to generate VPS26C phylogeny (consistent with Figure 7)

REFERENCES

Clough, S.J. and Bent, A.F. (1998) Floral dip: a simplified method for Agrobacterium-mediated transformation of *Arabidopsis thaliana*. *Plant J.* **16**, 735–743.

Collins, B.M., Norwood, S.J., Kerr, M.C., Mahony, D., Seaman, M.N., Teasdale, R.D. and Owen, D.J. (2008) Structure of VPS26B and mapping of its interaction with the retromer protein complex. *Traffic*, **9**, 366–379.

Edgar, A.J. and Polak, J.M. (2000) Human homologues of yeast vacuolar protein sorting 29 and 35. *Biochem. Biophys. Res. Commun.* **277**, 622–630.

Früholz, S. and Pimpl, P. (2017) Analysis of nanobody-epitope interactions in living cells via quantitative protein transport assays. *Methods Mol. Biol.* **1662**, 171–182.

Gallon, M. and Cullen, P.J. (2015) Retromer and sorting nexins in endosomal sorting. *Biochem. Soc. Trans.* **43**, 33–47.

Geldner, N., Friml, J., Stierhof, Y.-D., Jürgens, G. and Palme, K. (2001) Auxin transport inhibitors block PIN1 cycling and vesicle trafficking. *Nature*, **413**, 425–428.

Haft, C.R., de la Luz Sierra, M., Bafford, R., Lesniak, M.A., Barr, V.A. and Taylor, S.I. (2000) Human orthologs of yeast vacuolar protein sorting proteins Vps 26, 29, and 35: assembly into multimeric complexes. *Mol. Biol. Cell*, **11**, 4105–4116.

Halperin, S.J., Gilroy, S. and Lynch, J.P. (2003) Sodium chloride reduces growth and cytosolic calcium, but does not affect cytosolic pH, in root hairs of *Arabidopsis thaliana* L. *J. Exp. Bot.* **54**, 1269–1280.

Hashiguchi, Y., Niihama, M., Takahashi, T., Saito, C., Nakano, A., Tasaka, M. and Morita, M.T. (2010) Loss-of-function mutations of retromer large subunit genes suppress the phenotype of an Arabidopsis *zig* mutant that lacks Qb-SNARE VTI11. *Plant Cell*, **22**, 159–172.

Heard, W., Sklenář, J., Tomé, D.F., Robatzek, S. and Jones, A.M. (2015) Identification of regulatory and cargo proteins of endosomal and secretory pathways in Arabidopsis thaliana by proteomic dissection. *Mol. Cell Proteomics*, **14**, 1796–1813.

Horazdovsky, B.F., Davies, B.A., Seaman, M.N., McLaughlin, S.A., Yoon, S. and Emr, S.D. (1997) A sorting nexin-1 homologue, Vps5p, forms a complex with Vps17p and is required for recycling the vacuolar protein-sorting receptor. *Mol. Biol. Cell*, **8**, 1529–1541.

Jaillais, Y., Fobis-Loisy, I., Miege, C., Rollin, C. and Gaude, T. (2006) AtSNX1 defines an endosome for auxin-carrier trafficking in Arabidopsis. *Nature*, **443**, 106–109.

Jaillais, Y., Santambrogio, M., Rozier, F., Fobis-Loisy, I., Miège, C. and Gaude, T. (2007) The retromer protein VPS29 links cell polarity and organ initiation in plants. *Cell*, **130**, 1057–1070.

Jaillais, Y., Fobis-Loisy, I., Miège, C. and Gaude, T. (2008) Evidence for a sorting endosome in Arabidopsis root cells. *Plant J.* **53**, 237–247.

Kang, H., Kim, S.Y., Song, K., Sohn, E.J., Lee, Y., Lee, D.W., Hara-Nishimura, I. and Hwang, I. (2012) Trafficking of vacuolar proteins: the crucial role of Arabidopsis vacuolar protein sorting 29 in recycling vacuolar sorting receptor. *Plant Cell*, **24**, 5058–5073.

Kearse, M., Moir, R., Wilson, A. *et al.* (2012) Geneious Basic: an integrated and extendable desktop software platform for the organization and analysis of sequence data. *Bioinformatics*, **28**, 1647–1649. https://www.geneious.com

Kerr, M.C., Bennetts, J.S., Simpson, F., Thomas, E.C., Flegg, C., Gleeson, P.A., Wicking, C. and Teasdale, R.D. (2005) A novel mammalian retromer component, Vps26B. *Traffic*, **6**, 991–1001.

Kim, E., Lee, Y., Lee, H.J. *et al.* (2010) Implication of mouse Vps26b-Vps29-Vps35 retromer complex in sortilin trafficking. *Biochem. Biophys. Res. Commun.* **403**, 167–171.

Kleine-Vehn, J., Dhonukshe, P., Sauer, M., Brewer, P.B., Wiśniewska, J., Paciorek, T., Benková, E. and Friml, J. (2008a) ARF GEF-dependent transcytosis and polar delivery of PIN auxin carriers in Arabidopsis. *Curr. Biol.* **8**, 526–531.

Kleine-Vehn, J., Langowski, L., Wisniewska, J., Dhonukshe, P., Brewer, P.B. and Friml, J. (2008b) Cellular and molecular requirements for polar PIN targeting and transcytosis in plants. *Mol. Plant*, **1**, 1056–1066.

Koumandou, V.L., Klute, M.J., Herman, E.K., Nunez-Miguel, R., Dacks, J.B. and Field, M.C. (2011) Evolutionary reconstruction of the retromer complex and its function in *Trypanosoma brucei*. *J. Cell Sci.* **124**, 1496–1509.

Kudla, J. and Bock, R. (2016) Lighting the way to protein-protein interactions: recommendations on best practices for bimolecular fluorescence complementation analyses. *Plant Cell*, **28**, 1002–1008.

Künzl, F., Früholz, S., Fäßler, F., Li, B. and Pimpl, P. (2016) Receptor-mediated sorting of soluble vacuolar proteins ends at the trans-Golgi network/early endosome. *Nat. Plants*, **2**, 16017.

Kvainickas, A., Jimenez-Orgaz, A., Nägele, H., Hu, Z., Dengjel, J. and Steinberg, F. (2017) Cargo-selective SNX-BAR proteins mediate retromer trimer independent retrograde transport. *J. Cell Biol.* **216**, 3677–3693.

Larson, E.R., Domozych, D.S. and Tierney, M.L. (2014a) SNARE VTI13 plays a unique role in endosomal trafficking pathways associated with the vacuole and is essential for cell wall organization and root hair growth in arabidopsis. *Ann. Bot.* **114**, 1147–1159.

Larson, E.R., Tierney, M.L., Tinaz, B. and Domozych, D.S. (2014b) Using monoclonal antibodies to label living root hairs: a novel tool for studying cell wall microarchitecture and dynamics in Arabidopsis. *Plant Methods*, **10**, 30.

McNally, K.E., Faulkner, R., Steinberg, F. *et al.* (2017) Retriever is a multiprotein complex for retromer-independent endosomal cargo recycling. *Nat. Cell Biol.* **19**, 1214–1225.

Miller, M.A., Pfeiffer, W. and Schwartz, T. (2010) Creating the CIPRES Science Gateway for inference of large phylogenetic trees. In *2010 Gateway Computing Environments Workshop (GCE)*, New Orleans, LA, pp. 1–8.

Munch, D., Teh, O.-K., Malinovsky, F.G. *et al.* (2015) Retromer contributes to immunity-associated cell death in Arabidopsis. *Plant Cell*, **27**, 463–479.

Murashige, T. and Skoog, F. (1962) A revised medium for rapid growth and bio assays with tobacco tissue cultures. *Physiol. Plant.*, **15**, 473–497.

Niemes, S., Langhans, M., Viotti, C., Scheuring, D., San Wan Yan, M., Jiang, L., Hillmer, S., Robinson, D.G. and Pimpl, P. (2010) Retromer recycles vacuolar sorting receptors from the trans-Golgi network. *Plant J.* **61**, 107–121.

Nodzyński, T., Feraru, M.I., Hirsch, S., De Rycke, R., Niculaes, C., Boerjan, W., Van Leene, J., De Jaeger, G., Vanneste, S. and Friml, J. (2013) Retromer subunits VPS35A and VPS29 mediate prevacuolar compartment (PVC) function in Arabidopsis. *Mol. Plant*, **6**, 1849–1862.

Nothwehr, S.F. and Hindes, A.E. (1997) The yeast VPS5/GRD2 gene encodes a sorting nexin-1-like protein required for localizing membrane proteins to the late Golgi. *J. Cell Sci.* **110**, 1063–1072.

Oliviusson, P., Heinzerling, O., Hillmer, S., Hinz, G., Tse, Y.C., Jiang, L. and Robinson, D.G. (2006) Plant retromer, localized to the prevacuolar compartment and microvesicles in Arabidopsis, may interact with vacuolar sorting receptors. *Plant Cell*, **18**, 1239–1252.

Ovecka, M., Lang, I., Baluska, F., Ismail, A., Illes, P. and Lichtscheidl, I.K. (2005) Endocytosis and vesicle trafficking during tip growth of root hairs. *Protoplasma*, **226**, 39–54.

Paravicini, G., Horazdovsky, B.F. and Emr, S.D. (1992) Alternative pathways for the sorting of soluble vacuolar proteins in yeast: a vps35 null mutant missorts and secretes only a subset of vacuolar hydrolases. *Mol. Biol. Cell*, **3**, 415–427.

Peyroche, A., Antonny, B., Robineau, S., Acker, J., Cherfils, J. and Jackson, C.L. (1999) Brefeldin A acts to stabilize an abortive ARF–GDP–Sec7 domain protein complex: involvement of specific residues of the Sec7 domain. *Mol. Cell*, **3**, 275–285.

Pourcher, M., Santambrogio, M., Thazar, N., Thierry, A.M., Fobis-Loisy, I., Miège, C., Jaillais, Y. and Gaude, T. (2010) Analyses of sorting nexins reveal distinct retromer-subcomplex functions in development and protein sorting in Arabidopsis thaliana. *Plant Cell*, **22**, 3980–3991.

Preuss, M.L., Schmitz, A.J., Thole, J.M., Bonner, H.K., Otegui, M.S. and Nielsen, E. (2006) A role for the RabA4b effector protein PI-4Kβ1 in polarized expansion of root hair cells in *Arabidopsis thaliana*. *J. Cell Biol.* **172**, 991–998.

Rambaut, A. and Drummond, A.J. (2007) *Tracer*. Version 1.5. http://beast.bio.ed.ac.uk/Tracer

Richter, S., Geldner, N., Schrader, J., Wolters, H., Stierhof, Y.D., Rios, G., Koncz, C., Robinson, D.G. and Jürgens, G. (2007) Functional diversification of closely related ARF-GEFs in protein secretion and recycling. *Nature*, **448**, 488–492.

Richter, S., Müller, L.M., Stierhof, Y.D., Mayer, U., Takada, N., Kost, B., Vieten, A., Geldner, N., Koncz, C. and Jürgens, G. (2011) Polarized cell growth in Arabidopsis requires endosomal recycling mediated by GBF1-related ARF exchange factors. *Nat. Cell Biol.* **14**, 80–86.

Robinson, D.G. and Neuhaus, J.M. (2016) Receptor-mediated sorting of soluble vacuolar proteins: myths, facts, and a new model. *J. Exp. Bot.* **67**, 4435–4449.

Ronquist, F., Teslenko, M., van der Mark, P., Ayres, D.L., Darling, A., Höhna, S., Larget, B., Liu, L., Suchard, M.A. and Huelsenbeck, J.P. (2012) MrBayes 3.2: efficient Bayesian phylogenetic inference and model choice across a large model space. *Syst. Biol.* **61**, 539–542.

Sanderfoot, A.A., Kovaleva, V., Bassham, D.C. and Raikhel, N.V. (2001) Interactions between syntaxins identify at least five SNARE complexes within the Golgi/prevacuolar system of the Arabidopsis cell. *Mol. Biol. Cell*, **12**, 3733–3743.

Sanmartín, M., Ordóñez, A., Sohn, E.J., Robert, S., Sánchez-Serrano, J.J., Surpin, M.A., Raikhel, N.V. and Rojo, E. (2007) Divergent functions of VTI12 and VTI11 in trafficking to storage and lytic vacuoles in Arabidopsis. *Proc. Natl Acad. Sci. USA*, **104**, 3645–3650.

Seaman, M.N., Marcusson, E.G., Cereghino, J.L. and Emr, S.D. (1997) Endosome to Golgi retrieval of the vacuolar protein sorting receptor, Vps10p, requires the function of the VPS29, VPS30, and VPS35 gene products. *J. Cell Biol.* **137**, 79–92.

Simonetti, B., Danson, C.M., Heesom, K.J. and Cullen, P.J. (2017) Sequence-dependent cargo recognition by SNX-BARs mediates retromer-independent transport of CI-MPR. *J. Cell Biol.* **216**, 3695–3712.

Singh, M.K., Kruger, F., Beckmann, H., Brumm, S., Vermeer, J.E.M., Munnik, T., Mayer, U., Stierhof, Y.-D., Grefen, C. and Schumacher, K. (2014) Protein delivery to vacuole requires SAND protein-dependent Rab GTPase conversion for MVB-vacuole fusion. *Curr. Biol.* **24**, 1383–1389.

Stevens, P.F. (2001) Angiosperm phylogeny website. Version 12, July 2012. http://www.mobot.org/MOBOT/research/APweb/

Surpin, M., Zheng, H., Morita, M.T. *et al.* (2003) The VTI family of SNARE proteins is necessary for plant viability and mediates different protein transport pathways. *Plant Cell*, **15**, 2885–2899.

Takac, T., Pechan, T., Samajova, O., Ovecka, M., Richter, H., Eck, C., Niehaus, K. and Samaj, J. (2012) Wortmannin treatment induces changes in Arabidopsis root proteome and post-Golgi compartments. *J. Proteome Res.* **11**, 3127–3142.

Thazar-Poulot, N., Miquel, M., Fobis-Loisy, I. and Gaude, T. (2015) Peroxisome extensions deliver the Arabidopsis SDP1 lipase to oil bodies. *Proc. Natl Acad. Sci. USA*, **112**, 4158–4163.

Voigt, B., Timmers, A.C., Šamaj, J. *et al.* (2005) Actin-based motility of endosomes is linked to the polar tip growth of root hairs. *Eur. J. Cell Biol.* **84**, 609–621.

Wang, Y., Zhang, W., Li, K., Sun, F., Han, C., Wang, Y. and Li, X. (2008) Salt-induced plasticity of root hair development is caused by ion disequilibrium in *Arabidopsis thaliana*. *J. Plant. Res.* **121**, 87–96.

Yamazaki, M., Shimada, T., Takahashi, H., Tamura, K., Kondo, M., Nishimura, M. and Hara-Nishimura, I. (2008) Arabidopsis VPS35, a retromer component, is required for vacuolar protein sorting and involved in plant growth and leaf senescence. *Plant Cell Physiol.* **49**, 142–156.

Yano, D., Sato, M., Saito, C., Sato, M.H., Morita, M.T. and Tasaka, M. (2003) A SNARE complex containing SCR3/AtVAM3 and ZIG/VTI11 in gravity-sensing cells is important for Arabidopsis shoot gravitropism. *Proc. Natl Acad. Sci. USA*, **100**, 8589–8594.

Zelazny, E., Santambrogio, M., Pourcher, M., Chambrier, P., Berne-Dedieu, A., Fobis-Loisy, I., Miege, C., Jallais, Y. and Gaude, T. (2013) Mechanisms governing the endosomal membrane recruitment of the core retromer in Arabidopsis. *J. Biol. Chem.* **288**, 8815–8825.

Zhang, X., Henriques, R., Lin, S.S., Niu, Q.W. and Chua, N.H. (2006) Agrobacterium-mediated transformation of *Arabidopsis thaliana* using the floral dip method. *Nat. Protocols*, **1**, 641–646.

Zheng, H., von Mollard, G.F., Kovaleva, V., Stevens, T.H. and Raikhel, N.V. (1999) The plant vesicle-associated SNARE AtVTI1a likely mediates vesicle transport from the trans-Golgi network to the prevacuolar compartment. *Mol. Biol. Cell*, **10**, 2251–2264.

